Updated Upper Limits on the Isotropic Gravitational-Wave Background from LIGO, Virgo, and KAGRA Data through April 2025

A. G. Abac,[1] A. Abe,[2] I. Abouelfettouh,[3] F. Acernese,[4,5] K. Ackley,[6] A. Adam,[7] S. Adhicary,[8] D. Adhikari,[9,10] R. X. Adhikari,[11] V. K. Adkins,[12] S. Afroz,[13] A. Agapito,[14] D. Agarwal,[15] M. Agathos,[16] N. Aggarwal,[17] S. Aggarwal,[18] O. D. Aguiar,[19] I.-L. Ahrend,[20] L. Aiello,[21,22] A. Ain,[23] P. Ajith,[24] T. Akutsu,[25,26] L. Albers,[27] W. Ali,[28,29] S. Al-Kershi,[9,10] C. Allene,[30] A. Allocca,[31,5] S. Al-Shammari,[32] J. A. Alvarez,[33] S. Alvarez-Lopez,[34] W. Amar,[35] O. Amarasinghe,[32] A. Amato,[36,37] F. Amicucci,[38,39] C. Amra,[40] A. B. Anand,[33] C. Anand,[41] A. Ananyeva,[11] S. B. Anderson,[11] W. G. Anderson,[11] M. Andia,[42] M. Ando,[43,44] F. Andrade-Oliveira,[45] M. Andrés-Carcasona,[34] J. L. Andrey,[46] T. Andrić,[47,48] J. Anglin,[49] J. Anna,[50] J. M. Antelis,[51] S. Antier,[42] T. Aoki,[52] M. Aoumi,[53] E. Z. Appavuravther,[9,10] E. A. Appelt,[54] S. Appert,[11] S. K. Apple,[55] K. Arai,[11] A. Araya,[56] M. C. Araya,[11] F. Arciprete,[21,22] J. S. Areeda,[57] N. Aritomi,[58] F. Armato,[28,29] S. Armstrong,[59] N. Arnaud,[60] M. Arogeti,[61] S. M. Aronson,[49] G. Ashton,[62] Y. Aso,[53,63] L. Asprea,[64] M. Assiduo,[65,66] S. Assis de Souza Melo,[67] S. M. Aston,[68] P. Astone,[38] P. S. Aswathi,[69] F. Attadio,[39,38] F. Aubin,[70] K. AultONeal,[50] G. Avallone,[4] N. Avdeev,[64] E. A. Avila,[51] S. Babak,[20] C. Badger,[71] S. Bae,[72] S. Bagnasco,[64] S. Baimukhametova,[73,74] L. Baiotti,[75] T. Baka,[76,37] K. A. Baker,[7] T. Baker,[77] G. Balbi,[78] G. Baldi,[79,80] N. Baldicchi,[81,82] M. Ball,[83] G. Ballardin,[67] M. Ballelli,[47,48] S. W. Ballmer,[84] S. Banagiri,[41] B. Banerjee,[47] D. Bankar,[85] T. M. Baptiste,[12] P. Baral,[86] M. Baratti,[87,88] J. C. Barayoga,[11] K. Baric,[11] B. C. Barish,[11] D. Barker,[3] N. Barman,[85] F. Barone,[89,5] B. Barr,[90] M. Barrios,[33] L. Barsotti,[34] M. Barsuglia,[20] D. Barta,[91] M. A. Barton,[90] I. Bartos,[49] A. Basalaev,[9,10] R. Bassiri,[92] A. Basti,[88,87] M. Bawaj,[81,82] J. C. Bayley,[90] A. C. Baylor,[86] P. A. Baynard II,[61] M. Bazzan,[93,94] V. M. Bedakihale,[95] F. Beirnaert,[96] M. Bejger,[97] A. S. Bell,[90] C. Bellani,[98] D. S. Bellie,[99] D. Beltran-Martinez,[100] E. Benedetti,[38] W. Benoit,[18] I. Bentara,[60] M. Ben Yaala,[59] S. Bera,[101] F. Bergamin,[32] B. K. Berger,[92] M. Beroiz,[11] I. Berry,[102] D. Bersanetti,[28] T. Bertheas,[103] A. Bertolini,[37,36] J. Betzwieser,[68] D. Beveridge,[7] N. Bevins,[104] J. Bezerra-Sobrinho,[105] R. Bhandare,[106] R. Bhatt,[11] A. Bhattacharjee,[107] D. Bhattacharjee,[108,109] S. Bhattacharyya,[110] S. Bhaumik,[111] V. Biancalana,[112] F. Bianchi,[82] I. A. Bilenko,[113] M. Bilicki,[114] G. Billingsley,[11] A. Binetti,[98] S. Bini,[11] S. Biot,[115] O. Birnholtz,[116] S. Biscoveanu,[117] A. Bisht,[10] M. Bitossi,[67,87] M.-A. Bizouard,[118] S. Blaber,[119] J. K. Blackburn,[11] L. A. Blagg,[120] C. D. Blair,[7,68] D. G. Blair,[7] M. Bloch,[121] N. Bode,[9,10] N. Boettner,[27] P. Bogdan,[122] G. Boileau,[118] M. Boldrini,[67] G. N. Bolingbroke,[123] L. D. Bonavena,[49] V. A. Bonhomme,[34] E. Bonilla,[92] M. S. Bonilla,[57] A. Bonino,[83] R. Bonnand,[35,124] A. Borchers,[9,10] N. Borghi,[125,78] V. Boschi,[87] S. Bose,[126] V. Bossilkov,[68] Y. Bothra,[37,127] A. Boudon,[60] T. D. Boybeyi,[18] M. Boyle,[128] A. Bozzi,[67] C. Bradaschia,[87] M. J. Brady,[129] P. R. Brady,[86] A. Branch,[68] M. Branchesi,[47,48] T. Briant,[130] A. Brillet,[118,*] M. Brinkmann,[9,10] P. Brockill,[86] E. Brockmueller,[9,10] A. F. Brooks,[11] D. D. Brown,[123] M. L. Brozzetti,[81,82] S. Brunett,[11] G. Bruno,[15] R. Bruntz,[122] J. Bryant,[131] Y. Bu,[132] F. Bucci,[66] A. Buchicchio,[39] A. Buggiani,[67] O. Bulashenko,[133,134] T. Bulik,[135] H. J. Bulten,[37] A. Buonanno,[136,1] K. Burtnyk,[3] R. Buscicchio,[137,138] N. Busdon,[93] D. Buskulic,[35] R. L. Byer,[92] R. Cabrita,[15] V. A. Cáceres-Barbosa,[8] L. Cadonati,[61] G. Cagnoli,[93] C. Cahillane,[84] A. Calafat,[83] J. Calderón Bustillo,[139] J. D. Callaghan,[90] T. A. Callister,[140] E. Calloni,[31,5] S. R. Callos,[120] K. Cannon,[44] V. Cantory,[18] H. Cao,[34] L. A. Capistran,[141] E. Capocasa,[20] G. Capoccia,[82] E. Capote,[3] C. Capuano,[84] G. Capurri,[88,87] F. Carbognani,[67] K. J. Cardona-Martínez,[12] M. Carlassara,[9,10] M. Carpinelli,[137,67] G. Carrillo,[120] G. Carullo,[131] A. Casallas-Lagos,[142] J. Casanueva Diaz,[67] C. Casentini,[143,22] S. Caudill,[144] M. Cavaglià,[109] R. Cavalieri,[67] A. Ceja,[99] G. Cella,[87] P. Cerdá-Durán,[145,146] E. Cesarini,[22] N. Chabbra,[69] W. Chaibi,[118] A. Chakraborty,[13] P. Chakraborty,[9,10] S. Chakraborty,[106] S. Chalathadka Subrahmanya,[27] C. Chan,[147] J. C. L. Chan,[148] M. Chan,[119] C.-Y. Chang,[149] K. Chang,[150] S. Chao,[150] P. Charlton,[151] E. Chassande-Mottin,[20] C. Chatterjee,[54] Debarati Chatterjee,[85] Deep Chatterjee,[34] M. Chaturvedi,[106] S. Chaty,[20] A. Chen,[152] A. H.-Y. Chen,[153] D. Chen,[154] H. Chen,[149] H. Y. Chen,[155] S. Chen,[54] Yanbei Chen,[156] Yiwen Chen,[18] G. Cheng,[152] H. P. Cheng,[102] P. Chessa,[81,82] T. Cheunchitra,[132] H. T. Cheung,[157] S. Y. Cheung,[41] F. Chiadini,[158,159] G. Chiarini,[9,10] A. Chiba,[160] A. Chincarini,[28] D. Chintala,[108] A. Chiummo,[5,67] A. Chopra,[47] C. Chou,[161] S. Choudhary,[7] N. Christensen,[118,162] Y. K. Chu,[86] S. S. Y. Chua,[69] G. Ciani,[79,80] P. Ciecielag,[97] M. Cieślar,[135] M. Cifaldi,[22] B. Cirok,[163] F. Clara,[3] J. A. Clark,[11,61] T. A. Clarke,[117] A. Claveus,[164] M. R. Claypool,[120] S. Clesse,[115] F. Cleva,[118] S. M. Clyne,[129] E. Coccia,[47,48,165]

E. Codazzo,[166] P.-F. Cohadon,[130] D. E. Cohen,[9,10] E. Colangeli,[77] O. Cole,[147] M. Colleoni,[83] C. G. Collette,[167] J. Collins,[68] S. Colloms,[90] A. Colombo,[38,168] G. Compère,[115] C. M. Compton,[3] G. Connolly,[120] L. Conti,[94] T. R. Corbitt,[12] I. Cordero-Carrión,[169] S. Corezzi,[81,82] N. J. Cornish,[170] A. Corsi,[171] S. Cortese,[67] L. A. Corubolo,[21,22] L. Cotnoir,[122] R. Cottingham,[68] J. A. Cotturone,[99] M. W. Coughlin,[18] P. Couvares,[11,61] R. Coyne,[129] A. Cozzumbo,[47] J. D. E. Creighton,[86] T. D. Creighton,[172] S. Crook,[68] R. Crouch,[3] J. Csizmazia,[3] K. Csukás,[91] T. J. Cullen,[11] A. Cumming,[90] E. Cuoco,[125,78] M. Cusinato,[145] R. R. Cuzinatto,[173] L. V. da Conceição,[174] T. Dal Canton,[42] S. Dall'Osso,[78,125] S. Dal Pra,[175] G. Dálya,[103] Y. Dang,[8] B. D'Angelo,[28] S. Danilishin,[36,37] O. Danner,[107] S. D'Antonio,[38] K. Danzmann,[9,10] K. E. Darroch,[122] L. P. Dartez,[68] R. Das,[110] S. Das,[85] A. Dasgupta,[95] V. Dattilo,[67] A. Daumas,[20] I. Dave,[106] A. Davenport,[176] T. F. Davies,[7] D. Davis,[129] M. C. Davis,[18] P. Davis,[177,178] E. J. Daw,[179] M. Dax,[1] J. De Bolle,[96] E. deBruin,[18] M. Deenadayalan,[85] J. Degallaix,[180] M. De Laurentis,[31,5] C. J. Delgado Mendez,[100] F. De Lillo,[23] S. Della Torre,[138] W. Del Pozzo,[88,87] O. M. del Rio,[181] A. Demagny,[35] F. De Marco,[39,38] G. Demasi,[182,66] F. De Matteis,[21,22] C. de Melo,[173] N. Demos,[34] T. Dent,[139] A. Depasse,[15] N. DePergola,[104] R. De Pietri,[183,184] R. De Rosa,[31,5] C. De Rossi,[67] E. K. Derrick,[185] M. Desai,[34] D. DeSantis,[34] S. Deshmukh,[54] V. Deshmukh,[90] R. De Simone,[158,159] S. Determan,[186] S. Dhage,[15] A. Dhani,[1] R. Dhatri,[46] R. Dhurkunde,[77] R. Diab,[49] C. Diaz,[100] M. C. Díaz,[172] F. Diaz Guerra,[187,188] M. Di Cesare,[31,5] M. A. Dicorato,[82,189] T. Dietrich,[1] C. Di Fronzo,[7] M. Di Giovanni,[190,87] D. Diksha,[37,36] J. Ding,[20,191] S. Di Pace,[39,38] I. Di Palma,[39,38] D. Di Piero,[187,188] F. Di Renzo,[66,182] Divyajyoti,[32] A. Dmitriev,[131] J. P. Docherty,[90] Z. Doctor,[99] N. Doerksen,[174] E. Dohmen,[3] A. Doke,[144] A. Domiciano De Souza,[192] L. D'Onofrio,[5] F. Donovan,[34] K. L. Dooley,[32] S. Doravari,[85] O. Dorosh,[193] F. Dosopoulou,[32] M. Drago,[39,38] J. C. Driggers,[3] M. Dubois,[103] R. S. Dumbreck,[32] U. Dupletsa,[47] D. D'Urso,[194,166] P. Dutta Roy,[49] H. Duval,[195] S. Dwivedi,[196] S. E. Dwyer,[3] C. Eassa,[3] M. Eberhardt,[186] M. Ebersold,[45] M. Ebiri,[197] G. Eddolls,[84] A. Effler,[68] J. Eichholz,[131] H. Einsle,[118] M. Eisenmann,[25] M. Emma,[62] K. Endo,[160] R. Enficiaud,[1] V. Ernst,[15,198] L. Errico,[31,5] R. Espinosa,[172] M. Esposito,[5,31] R. C. Essick,[199] H. Estellés,[83] T. Etzel,[11] M. Evans,[34] T. Evstafyeva,[200] J. M. Ezquiaga,[148] F. Fabrizi,[65,66] V. Fafone,[21,22] S. Fairhurst,[32] X. Fan,[152] A. M. Farah,[199] B. Farr,[120] W. M. Farr,[201,202] M. Favata,[203] M. Fays,[198] M. Fazio,[59] J. Feicht,[11] M. M. Fejer,[92] J.-N. Feldhusen,[27] E. Fenyvesi,[91,204] A. Feo,[183,184] J. Fernandes,[111] T. Fernandes,[205,145] G. Fernández Rodríguez,[169] D. Fernando,[197] S. Ferraiuolo,[206,39,38] T. A. Ferreira,[19] M. Ferrer-Martinez,[83] F. Fidecaro,[88,87] P. Figura,[97] I. Fiori,[67] M. Fishbach,[199] R. P. Fisher,[122] S. K. Fitzgerald,[90] V. Fiumara,[207,159] R. Flaminio,[35] B. Flanagan,[32] S. M. Fleischer,[181] L. S. Fleming,[208] F. Flocco,[93] E. Floden,[18] H. Fong,[119] J. A. Font,[145,146] F. Fontinele-Nunes,[18] C. Foo,[1] B. Fornal,[209] P. W. F. Forsyth,[69] A. Fragkos,[210,74] N. Franchini,[211] A. Franco-Ordovas,[11] F. Frappez,[35] F. Frasconi,[87] J. P. Freed,[50] Z. Frei,[212] A. Freise,[37,127] O. Freitas,[205,145] R. Frey,[120] W. Frischhertz,[68] P. Fritschel,[34] V. V. Frolov,[68] M. Fuentes-Garcia,[11] R. Fujii,[160] T. Fujimori,[2] Y. Fujiwara,[213] P. Fulda,[49] M. Fyffe,[68] J. R. Gair,[1] S. Galaudage,[192] V. Galdi,[214] M. Galimberti,[67] A. Gamboa,[1] S. Gamoji,[215] A. Ganguly,[85] B. Garaventa,[28] P. García Abia,[100] J. García-Bellido,[216] C. García-Quirós,[83] J. W. Gardner,[69] S. Garg,[44] J. Gargiulo,[67] X. Garrido,[42] A. Garron,[83] F. Garufi,[31,5] P. A. Garver,[92] C. Gasbarra,[217,22] F. Gautier,[218] V. Gayathri,[86] T. Gayer,[84] G. Gemme,[28] A. Gennai,[87] V. Gennari,[103] J. George,[106] R. George,[155] O. Gerberding,[27] L. Gergely,[163] A. Ghinassi,[125,78] Archisman Ghosh,[96] Sayantan Ghosh,[111] Shaon Ghosh,[203] Shrobana Ghosh,[9,10] Suprovo Ghosh,[219] Tathagata Ghosh,[85,220] J. A. Giaime,[12,68] K. D. Giardina,[68] D. R. Gibson,[208] C. Gier,[59] F. Gittins,[76] J. Glanzer,[11] F. Glotin,[42] E. Glowacki,[221] J. Godfrey,[120] R. V. Godley,[9,10] O. Godwin,[11] A. S. Goettel,[222] E. Goetz,[119] J. Golomb,[11] S. Gomez Lopez,[39,38] G. González,[12] P. Goodarzi,[46] S. R. Goode,[41] A. Goodwin-Jones,[15] M. Gosselin,[67] S. M. Goss-Grubbs,[18] C. Gostiaux,[70] R. Gouaty,[35] D. W. Gould,[69] D. Goupilliere,[178,177] K. Govorkova,[34] A. Grado,[81,82] V. Graham,[90] A. E. Granados,[18] M. Granata,[180] V. Granata,[223,159] S. Gras,[34] P. Grassia,[11] C. Gray,[3] R. Gray,[90] G. Greco,[82] A. C. Green,[37,36] L. Green,[224] S. R. Green,[222] A. M. Gretarsson,[50] E. M. Gretarsson,[50] D. Griffith,[11] C. Grimaud,[35] H. Grote,[32] S. Grunewald,[1] A. G. Guerrero,[225] G. M. Guidi,[65,66] T. Guidry,[3] H. K. Gulati,[95] F. Gulminelli,[177,178] H. Guo,[152] W. Guo,[7] Y. Guo,[37] A. Gupta,[226] I. Gupta,[99] N. C. Gupta,[95] S. K. Gupta,[49] V. Gupta,[18] N. Gupte,[1] N. Guttman,[41] F. Guzman,[141] M. Haberland,[1] S. Haino,[227] E. D. Hall,[34] E. Z. Hamilton,[83] G. Hammond,[90] W.-B. Han,[228] M. Haney,[37] J. Hanks,[3] C. Hanna,[8] M. D. Hannam,[32] O. A. Hannuksela,[229] H. Hansen,[3] J. Hanson,[68] R. Harada,[44] A. R. Hardison,[186] S. Harikumar,[97] K. Haris,[230] I. Harley-Trochimczyk,[141] J. Harms,[47,48] G. M. Harry,[231]

I. W. Harry,[77] M. T. Hartman,[40,232,20] B. Haskell,[233,234] C.-J. Haster,[224] K. Haughian,[90] H. Hayakawa,[53] K. Hayama,[235] J. Hedberg,[50] A. Heffernan,[83] D. Hegde,[15] M. C. Heintze,[68] J. Heinzel,[34] H. Heitmann,[118] F. Hellman,[33] A. F. Helmling-Cornell,[185] G. Hemming,[67] O. Henderson-Sapir,[123] M. Hendry,[90] I. S. Heng,[90] M. H. Hennig,[90] C. Henshaw,[61] A. Heranval,[8] M. Heurs,[9,10] A. L. Hewitt,[236,237] J. Heynen,[15] J. Heyns,[34] S. Hido,[220] S. Hild,[36,37] M. Hill,[122] S. Hill,[90] Y. Himemoto,[238] C. Hirose,[53] D. Hofman,[180] N. A. Holland,[11] K. Holley-Bockelmann,[54] I. J. Hollows,[179] D. E. Holz,[225] L. Honet,[115] K. M. Hoops,[215] M. E. Hoque,[239] D. J. Horton-Bailey,[33] J. Hough,[90] S. Hourihane,[11] N. T. Howard,[54] E. J. Howell,[7] C. G. Hoy,[77] P. Hsi,[34] H.-Y. Hsieh,[240] C. Hsiung,[241] S.-H. Hsu,[242] W.-F. Hsu,[98] H. Y. Huang,[150] Y. Huang,[8] A. D. Huddart,[243] B. Hughey,[50] D. C. Y. Hui,[244] S. Husa,[83] L. Iampieri,[39,38] G. A. Iandolo,[36] M. Ianni,[22,21] Y. Ichinose,[220] K. Ide,[213] R. Iden,[245] A. Ierardi,[47,48] S. Ikeda,[154] H. Imafuku,[44] K. Imai,[220] Y. Inoue,[150] P. Iosif,[187,188] J. Irwin,[90,76] K. Ishida,[2] R. Ishikawa,[213] T. Ishikawa,[52] H. Ishino,[2] M. Isi,[246,202] K. S. Isleif,[247] Y. Itoh,[2,248] S. Iwaguchi,[52] M. M. Iwaya,[32,220] B. R. Iyer,[24] C. Jacquet,[103] T. Jacquot,[42] S. J. Jadhav,[249] S. P. Jadhav,[147] K. Jain,[32] A. L. James,[11] K. Jani,[54] S. Jani,[18] J. Janquart,[15,250] N. N. Janthalur,[249] S. Jaraba,[251] P. Jaranowski,[221] R. Jaume,[83] W. Javed,[32] M. Jensen,[3] W. Jia,[34] J. Jiang,[102] H.-B. Jin,[252,253] S.-J. Jin,[7] G. R. Johns,[122] N. A. Johnson,[49] M. C. Johnston,[224] R. Johnston,[90] N. Johny,[9,10] D. H. Jones,[69] D. I. Jones,[219] R. Jones,[90] P. Joshi,[61] S. K. Joshi,[85] G. Joubert,[60] J. Ju,[254] L. Ju,[7] I. L. Juarez-Reyes,[120] K. Jung,[255] H. B. Kabagoz,[34] B. Kacskovics,[91] T. Kajita,[220] I. Kaku,[2] V. Kalogera,[99] M. Kalomenopoulos,[224] M. Kamiizumi,[53] N. Kanda,[248,2] S. Kandhasamy,[85] G. Kang,[256] J. B. Kanner,[11] S. J. Kapadia,[85] D. P. Kapasi,[57] A. Karia,[37,127] A. S. Karia,[257] R. Kashyap,[111] M. Kasprzack,[11] H. Kato,[160] T. Kato,[220] E. Katsavounidis,[34] W. Katzman,[68] R. Kaushik,[106] K. Kawabe,[3] S. Kawamura,[52] D. Keitel,[83] S. A. Kemper,[55] L. J. Kemperman,[123] J. Kennington,[8] R. Kesharwani,[85] J. S. Key,[258] R. Khadela,[9,10] S. S. Khadkikar,[8] F. Y. Khalili,[113] C. Khamar,[199] F. Khan,[9,10] M. Khursheed,[106] N. M. Khusid,[201,202] W. Kiendrebeogo,[259] C. Kim,[260] G. Kim,[261] J. C. Kim,[262] K. Kim,[263] M. H. Kim,[254] S. Kim,[244] Y.-M. Kim,[263] C. Kimball,[99] K. Kimes,[57] M. Kinnear,[32] J. S. Kissel,[3] S. Klimenko,[49] A. M. Knee,[157] N. Knust,[9,10] K. Kobayashi,[220] S. M. Koehlenbeck,[92] K. Kohri,[264] K. Kokeyama,[32,52] S. Koley,[47,198] P. Kolitsidou,[83] A. E. Koloniari,[265] K. Komori,[25,43] K. Kompanets,[18] A. K. H. Kong,[266] A. Kontos,[185] K. Kopczuk,[108] L. M. Koponen,[131] M. Korobko,[27] X. Kou,[18] N. Kouvatsos,[71] T. Koyama,[160] D. B. Kozak,[11] E. Kraja,[67] S. L. Kranzhoff,[36,37] V. Kringel,[9,10] N. V. Krishnendu,[131] S. Kroker,[267] A. Królak,[268,193] K. Kruska,[9,10] J. Kubisz,[269] K. Kubota,[220] G. Kuehn,[9,10] D. Kukla,[18] A. Kulur Ramamohan,[69] Achal Kumar,[49] Anil Kumar,[249] Dhruv Kumar,[8,90] Praveen Kumar,[139] Prayush Kumar,[24] Rahul Kumar,[3] Rakesh Kumar,[95] Ravi Kumar,[18] J. Kume,[270,44] K. Kuns,[34] N. Kuntimaddi,[32] S. Kuroyanagi,[216,271,272] K. Kwak,[255] K. Kwan,[69] S. Kwon,[44] G. Lacaille,[90] D. Laghi,[45] A. H. Laity,[129] N. Lajili,[124,273] A. Lakhal,[130] E. Lalande,[274] M. Lalleman,[23] S. Lalvani,[99] M. Landry,[3] R. N. Lang,[34] A. Lange,[18] J. A. Lange,[64] R. Langgin,[224] B. Lantz,[92] I. La Rosa,[83] O. Laske,[8] P. D. Lasky,[41] L. Lavezzi,[64] J. Lawrence,[172] M. Laxen,[68] A. Lazzarini,[11] C. Lazzaro,[275,166] P. Leaci,[39,38] L. Leali,[18] Y. K. Lecoeuche,[119] H. W. Lee,[276] J. Lee,[84] K. Lee,[254] R.-K. Lee,[149] R. Lee,[34] Sungho Lee,[277] Sunjae Lee,[254] W. Lee,[255] Y. Lee,[150] F. Legger,[64] I. N. Legred,[11] J. Lehmann,[9,10] L. Lehner,[200] M. Le Jean,[180,124] A. Lemaître,[278] R. Lemrani Alaoui,[124,273] M. Lenti,[66,182] M. Leonardi,[79,80,279] M. Lequime,[40] M. Lesovsky,[11] N. Letendre,[35] M. Lethuillier,[60] Y. Levin,[41] S. Lexmond,[127] K. Leyde,[201,202] A. K. Y. Li,[44] K. L. Li,[280] T. G. F. Li,[98] X. Li,[156] Y. Li,[99] Z. Li,[90] Q. Liang,[152] C-Y. Lin,[281] E. T. Lin,[282] F. Lin,[150] L. C.-C. Lin,[280] Y.-C. Lin,[282] C. Lindsay,[208] S. D. Linker,[215] A. Liu,[229] F. Liu,[42] G. C. Liu,[241] Jian Liu,[7] S. Liu,[152] F. Llamas Villarreal,[172] J. Llobera-Querol,[83] R. K. L. Lo,[148] J.-P. Locquet,[98] S. C. G. Loggins,[164] L. T. London,[71] A. Longo,[65,66] M. Lopez Portilla,[76] A. Lorenzo-Medina,[139] V. Loriette,[42] M. Lormand,[68] M. Lorusso,[78] G. Losurdo,[190,87] T. P. Lott IV,[229] J. D. Lough,[9,10] H. A. Loughlin,[34] C. O. Lousto,[197] N. K. Y. Low,[132] N. Lu,[69] H. Lück,[9,10] O. Lukina,[34] D. Lumaca,[22] A. P. Lundgren,[283,284] L. Lunghini,[67] A. W. Lussier,[274] L.-T. Ma,[282] X. Ma,[46] M. Ma'arif,[150] S. MacBride,[45] K. Machida,[160] D. M. Macleod,[32] I. A. O. MacMillan,[11] A. Macquet,[42] S. S. Madekar,[165] S. Maenaut,[98] S. S. Magare,[85] R. M. Magee,[11] E. Maggio,[1,38] M. Magnozzi,[28,29] P. Mahapatra,[32] M. Mahesh,[27] S. Majhi,[85] E. Majorana,[39,38] C. N. Makarem,[11] E. Makelele,[108] N. Malagon,[197] D. Malakar,[109] J. A. Malaquias-Reis,[19] U. Mali,[199] S. Maliakal,[11] A. Malik,[106] L. Mallick,[174,199] A.-K. Malz,[62] N. Man,[118] M. Mancarella,[101] V. Mandic,[18] V. Mangano,[194,166] Z. Mangi,[197] B. Mannix,[120] G. L. Mansell,[84] M. Manske,[86] M. Mantovani,[67] M. Mapelli,[93,94,285] S. Marchetti,[93,94] F. Marion,[35] J. Mark,[18] A. S. Markosyan,[92] J. Markus,[18] E. Maros,[11] S. Marsat,[103] F. Martelli,[65,66]

I. W. Martin,[90] R. M. Martin,[203] B. B. Martinez,[141] M. Martinez,[165, 286] V. Martinez,[287] A. Martini,[79, 80] Juan Carlos Martins,[288] Julio C. Martins,[19] D. V. Martynov,[131] E. J. Marx,[34] L. Massaro,[36, 37] A. Masserot,[35] M. Masso-Reid,[90] T. Masters,[108] S. Mastrogiovanni,[38] G. Mastropasqua,[78] M. Matiushechkina,[9, 10] A. Matte-Landry,[274] L. Maurin,[218] N. Mavalvala,[34] N. Maxwell,[3] A. McCann,[120] G. McCarrol,[68] R. McCarthy,[3] D. E. McClelland,[69] S. McCormick,[68] L. McCuller,[11] L. I. McDermott,[126] C. McElhenny,[122] G. I. McGhee,[90] K. B. M. McGowan,[54] J. McIver,[119] A. McLeod,[7] I. McMahon,[45] T. McRae,[69] R. McTeague,[90] K. McWhirter,[8] D. Meacher,[86] B. N. Meagher,[84] R. Mechum,[197] L. G. Medeiros,[105] R. M. Mehta,[18] A. Melatos,[132] C. S. Menoni,[176] R. A. Mercer,[86] L. Mereni,[180] K. Merfeld,[120] E. L. Merilh,[68] J. R. Mérou,[83] C. Messick,[86] M. Meyer-Conde,[30] F. Meylahn,[9, 10] H. Miao,[289] C. Michel,[180] Y. Michimura,[44] H. Middleton,[131] D. P. Mihaylov,[108] S. J. Miller,[11] M. Millhouse,[61] E. Milotti,[187, 188] V. Milotti,[93] E. Minakaki,[127] Y. Minenkov,[22] Ll. M. Mir,[165] L. Mirasola,[290] C.-A. Miritescu,[165] A. Mishra,[24] C. Mishra,[110] T. Mishra,[77] A. Mitchell,[92] J. G. Mitchell,[50] O. Mitchem,[120] S. Mitra,[85] V. P. Mitrofanov,[113] K. Mitsuhashi,[25] R. Mittleman,[34] O. Miyakawa,[53] S. Miyoki,[53] G. Mo,[11] L. Mobilia,[65, 66] S. R. P. Mohapatra,[11] M. Molina-Ruiz,[33] M. Mondin,[215] M. Montani,[65, 66] G. Montefusco,[178] C. J. Moore,[236] D. Moraru,[3] A. More,[85] S. More,[85] C. Moreno,[291] E. A. Moreno,[34] G. Moreno,[3] A. Moreso Serra,[133] C. Morgan,[32] S. Morisaki,[220] S. Moriwaki,[220] Y. Moriwaki,[160] G. Morras,[216] A. Moscatello,[93] M. Mould,[222] B. Mours,[70] C. M. Mow-Lowry,[37, 127] L. Muccillo,[182, 66] F. Muciaccia,[39, 38] Arunava Mukherjee,[239] D. Mukherjee,[131] Samanwaya Mukherjee,[24] Soma Mukherjee,[172] Subroto Mukherjee,[95] Suvodip Mukherjee,[13] N. Mukund,[34] A. Mullavey,[68] C. L. Mungioli,[7] Y. Murakami,[220] M. Murakoshi,[213] P. G. Murray,[90] D. Nabari,[79, 80] S. Nadji,[180] A. Nagar,[64, 292] N. Nagarajan,[1] K. Nakagaki,[53] A. Nakamura,[52] K. Nakamura,[25] H. Nakano,[293] M. Nakano,[11] D. Nanadoumgar-Lacroze,[165] D. Nandi,[12] V. Napolano,[67] S. U. Naqvi,[110] P. Narayan,[226] A. Nardecchia,[39, 38] I. Nardecchia,[22] T. Narikawa,[220] H. Narola,[76] L. Naticchioni,[38] R. K. Nayak,[294] J. Neeson,[32] L. Negri,[76] A. Nela,[90] C. Nelle,[120] A. Nelson,[141] T. J. N. Nelson,[68] A. Nemmani,[97] A. Neunzert,[3] M. Newell,[16] S. Ng,[57] T. C. K. Ng,[37, 76] L.-A. T. Nguyen,[295] T. T. Nguyen,[295] L. Nguyen Quynh,[295] A. B. Nielsen,[296] Y. Nishino,[25, 297] A. Nishizawa,[298] S. Nissanke,[299, 37] W. Niu,[8] F. Nocera,[67] J. Noller,[300] M. Norman,[32] C. North,[32] J. Novak,[251, 301] G. Nurbek,[172] L. K. Nuttall,[77] K. Obayashi,[213] J. Oberling,[3] C. E. Ochoa,[46] C. O'Connor,[84] J. O'Dell,[243] E. Oelker,[34] M. Oertel,[251, 301] G. Oganesyan,[47, 48] J. J. Oh,[262] T. O'Hanlon,[68] M. Ohashi,[53, 30] F. Ohme,[9, 10] Y. Okabe,[160] I. Oke,[59] R. Oliveira,[302] R. Omer,[18] N. O'Neill,[84] M. Onishi,[160] K. Oohara,[303, 304] P. Ophardt,[247] R. J. Oram,[68] B. O'Reilly,[68] R. O'Shaughnessy,[197] S. Oshino,[53] J. Ostrovska,[131] A. Osumi,[52] I. Ota,[12] G. Othman,[247] M. Otsuka,[25, 297] D. J. Ottaway,[123] A. Ouzriat,[60] H. Overmier,[68] B. J. Owen,[107] A. E. Pace,[8] M. A. Page,[25] A. Pai,[111] S. Pal,[294] M. A. Palaia,[87, 88] M. Pálfi,[212] C. Palomba,[38] H. Pan,[266] J. Pan,[7] K.-C. Pan,[149, 282] P. K. Panda,[249] Shiksha Pandey,[8] Swadha Pandey,[34] P. T. H. Pang,[37, 76] F. Pannarale,[39, 38] B. C. Pant,[106] F. H. Panther,[7] M. Panzeri,[65, 66] F. Paoletti,[87] A. Paoli,[67] A. Paolone,[38, 305] A. Papadopoulos,[90] E. E. Papalexakis,[46] L. Papalini,[87, 88] G. Papigkiotis,[265] A. Paquis,[42] A. Parisi,[81, 82] B.-J. Park,[277] Jihwan Park,[260] Junegyu Park,[261] W. Parker,[68] G. Pascale,[9, 10] D. Pascucci,[96] A. Pasqualetti,[67] L. Passenger,[41] D. Passuello,[87] O. Patane,[3] A. V. Patel,[150] L. Pathak,[85] A. Patra,[32] B. Patricelli,[88, 87] B. G. Patterson,[32] K. Paul,[110, 37] S. Paul,[120] E. Payne,[11] T. Pearce,[32] M. Pedraza,[11] A. Pele,[11] F. E. Peña Arellano,[215] X. Peng,[131] Y. Peng,[61] S. Penn,[84, 306] A. Perreca,[47, 48] J. Perret,[20] D. Pesios,[265] S. Petracca,[214] C. Petrillo,[81] H. P. Pfeiffer,[1] H. Pham,[68] K. A. Pham,[18] K. S. Phukon,[131] H. Phurailatpam,[229] L. Piccari,[39, 38] O. J. Piccinni,[83] M. Pichot,[118] A. Pied,[90] M. Piendibene,[88, 87] F. Piergiovanni,[65, 66] L. Pierini,[38] G. Pierra,[38] V. Pierro,[307, 159] M. Pillas,[308, 42] B. Pillon,[50] L. Pinard,[180] I. M. Pinto,[307, 159, 309, 31] M. Pinto,[67] B. J. Piotrzkowski,[86] M. Pirello,[3] A. Pisarski,[221] M. D. Pitkin,[236, 90] E. Placidi,[39, 38] M. L. Planas,[1] C. Plunkett,[34] R. Poggiani,[88, 87] E. Polini,[118] M. Polo,[100] J. Pomper,[87, 88] L. Pompili,[222] J. Poon,[229] E. Porcelli,[37] A. S. Porter,[107] E. K. Porter,[20] C. Posnansky,[8] J. Powell,[147] G. S. Prabhu,[85] M. Pracchia,[198] A. K. Prajapati,[95] K. Prasai,[310] R. Prasanna,[249] P. Prasia,[311] G. Pratten,[131] G. Principe,[187, 188] G. A. Prodi,[79, 80] P. Prosperi,[87] P. Prosposito,[21, 22] A. Puecher,[1] J. Pullin,[12] M. Punturo,[82] P. Puppo,[38] M. Pürrer,[129] H. Qi,[16] M. Qiao,[152] J. Qin,[69] G. Quéméner,[178, 124] V. Quetschke,[172] P. J. Quinonez,[50] R. Rading,[247] I. Rainho,[145] S. Raja,[106] C. Rajan,[106] B. Rajbhandari,[107] M. R. Raj Sah,[13] K. E. Ramirez,[68] F. A. Ramis Vidal,[83] M. Ramos Arevalo,[172] A. Ramos-Buades,[83] S. Ranjan,[61] M. Ranjbar,[46] K. Ransom,[68] R. Rao,[152] P. Rapagnani,[39, 38] B. Ratto,[50] A. Ravichandran,[144] A. Ray,[99] V. Raymond,[32] M. Razzano,[88, 87] J. Read,[57] J. Redepenning,[18] J. Regan,[224] T. Regimbau,[35] T. Reichardt,[147] S. Reid,[59] C. Reissel,[34] D. H. Reitze,[11] A. I. Renzini,[45, 137, 138]

B. Revenu,[121,42] A. Revilla-Peña,[133] F. Ricci,[39,38] M. Ricci,[38,39] A. Ricciardone,[88,87] J. Rice,[84] J. W. Richardson,[46] M. L. Richardson,[34] K. Riles,[157] H. K. Riley,[32] A. Riminucci,[65,66] F. Robinet,[42] M. Robinson,[3] A. Rocchi,[22] J. Rodriguez,[84] R. Rodriguez Lopez,[176] L. Rolland,[35] J. G. Rollins,[11] A. E. Romano,[312] R. Romano,[4,5] A. Romero-Rodríguez,[35] I. M. Romero-Shaw,[32] J. H. Romie,[68] S. Ronchini,[8,47,48] T. J. Roocke,[123] T. J. Rosauer,[46] C. A. Rose,[61] D. Rosińska,[135] M. P. Ross,[55] M. Rossello-Sastre,[83] S. Rowan,[90] K. Rowlands,[186] S. K. Roy,[201,202] S. Roy,[15,250] T. RoyChowdhury,[86] D. Rozza,[137,138] P. Ruggi,[67] G. H. Ruiz,[164] E. Ruiz Morales,[313,216] K. Ruiz-Rocha,[54] V. Russ,[181] S. M. S,[230] S. Sachdev,[61] T. Sadecki,[3] F. Safai Tehrani,[38] P. Saffarieh,[37,127] S. Safi-Harb,[174] S. Saha,[282] T. Sainrat,[20] S. Sajith Menon,[314,39,38] K. Sakai,[315] Y. Sakai,[30] M. Sakellariadou,[71] S. Sakon,[8] F. Salces-Carcoba,[11] L. Salconi,[67] M. Saleem,[155] F. Salemi,[39,38] M. Sallé,[37] M. Salomé,[60] S. U. Salunkhe,[85] S. Salvador,[178,177] A. Salvarese,[155] A. Samajdar,[76,37] P. M. Samir,[185] A. Sanchez,[3] E. J. Sanchez,[11] J. Sanchez,[68] D. Sanchez-Cid,[45] N. Sanchis-Gual,[145] J. R. Sanders,[186] E. M. Sänger,[1] F. Santoliquido,[47,48] E. Sapkin,[41] F. Sarandrea,[64] T. R. Saravanan,[85] P. Sarkar,[9,10] A. Sasli,[18] P. Sassi,[82,81] B. Sassolas,[180] O. Sauter,[49] R. L. Savage,[3] T. Savicheva,[176] T. Sawada,[53] H. L. Sawant,[85] D. Schaetzl,[11] M. Scheel,[156] A. Schiebelbein,[199] M. G. Schiworski,[84] K. Schluterman,[50] P. Schmidt,[131] R. Schnabel,[27] M. Schneewind,[9,10] R. M. S. Schofield,[120,3] M. Schoor,[35] K. Schouteden,[98] B. W. Schulte,[9,10] M. Schulz,[47,48] B. F. Schutz,[32,9,10] E. Schwartz,[196] M. Scialpi,[316] J. Scott,[90] S. M. Scott,[69] R. M. Sedas,[68] T. C. Seetharamu,[90] M. Seglar-Arroyo,[165] Y. Sekiguchi,[317] D. Sellers,[68] N. Sembo,[2] E. G. Seo,[90] J. W. Seo,[98] G. Seong,[260] V. Sequino,[31,5] M. Serra,[38] C. K. Sethi,[144] A. Sevrin,[195] T. Shaffer,[3] U. S. Shah,[61] M. A. Shaikh,[318] L. Shao,[319] J. Sharkey,[90] A. K. Sharma,[83] Preeti Sharma,[12] Priyanka Sharma,[106] Sushant Sharma-Chaudhary,[18] P. Shawhan,[136] T. Shen,[69] Z.-H. Shi,[149] K. Shimode,[53] H. Shinkai,[320] S. Shirke,[85] D. H. Shoemaker,[34] D. M. Shoemaker,[155] R. W. Short,[3] S. ShyamSundar,[106] H. Siegel,[200] V. Sierra,[291] D. Sigg,[3] L. Silenzi,[36,37] P. J. S. Silva,[288] L. Silvestri,[39,175] M. Simmonds,[123] L. P. Singer,[321] A. Singh,[226] D. Singh,[33] M. K. Singh,[32] N. Singh,[83] S. Singh,[245,25] M. R. Sinha,[41] A. M. Sintes,[83] V. Skliris,[32] B. J. J. Slagmolen,[69] T. J. Slaven-Blair,[7] J. Smetana,[131] D. A. Smith,[68] J. R. Smith,[57] J. Smith,[32] L. Smith,[187,188] W. J. Smith,[54] S. Soares de Albuquerque Filho,[65,66] M. Soares-Santos,[45] K. Somiya,[245] I. Song,[282] S. Soni,[46] V. Sordini,[60] F. Sorrentino,[28] H. Sotani,[322] N. E. Sovitzky,[323] F. Spada,[87] V. Spagnuolo,[37] A. P. Spencer,[90] M. Spera,[188,324] P. Spinicelli,[67] A. K. Srivastava,[95] F. Stachurski,[90] V. V. Stanford,[107] A. Stanton,[32] D. A. Steer,[325] N. Steinle,[174] J. Steinlechner,[36,37] S. Steinlechner,[36,37] C. Stephens,[32] N. Stergioulas,[265] M. StPierre,[129] J. Stremiz,[57] M. D. Strong,[12] A. Strunk,[3] M. Suchenek,[97] S. Sudhagar,[97] R. Sugimoto,[43] L. Suleiman,[57] K. D. Sullivan,[12] J. Sun,[262,79] L. Sun,[69] S. Sunil,[95] J. Suresh,[118] P. J. Sutton,[32] K. Suzuki,[245] M. Suzuki,[220] A. Svizzeretto,[81] B. L. Swinkels,[37] A. Syx,[124] M. J. Szczepańczyk,[142] M. Tacca,[37] M. Tagliazucchi,[125,78] H. Tagoshi,[220] S. C. Tait,[11] H. Takaba,[154] K. Takada,[220] H. Takahashi,[30] R. Takahashi,[25] A. Takamori,[56] S. Takano,[9,10] H. Takeda,[326,327] I. Takimoto Schmiegelow,[47,48] C. Talbot,[117] M. Tamaki,[220] N. Tamanini,[103] D. Tanabe,[150] K. Tanaka,[245] S. J. Tanaka,[213] S. Tanioka,[32] D. B. Tanner,[49] W. Tanner,[9,10] L. Tao,[46] R. D. Tapia,[8] E. N. Tapia San Martín,[37] A. Taruya,[328] J. D. Tasson,[162] J. G. Tau,[197] A. Tejera,[171] J. G. Temple,[108] Y. Teng,[86] H. Themann,[215] A. Theodoropoulos,[145] M. P. Thirugnanasambandam,[85] L. M. Thomas,[11] M. Thomas,[68] P. Thomas,[3] J. E. Thompson,[219] S. R. Thondapu,[106] E. Thrane,[41] J. Tissino,[47,48] A. Tiwari,[85] Pawan Tiwari,[47] Praveer Tiwari,[329] S. Tiwari,[45] V. Tiwari,[131] M. R. Todd,[84] E. Tofani,[38] M. Toffano,[93] A. M. Toivonen,[18] K. Toland,[90] T. Tomaru,[25] V. Tommasini,[11] H. Tong,[41] C. I. Torrie,[11] I. Tosta e Melo,[330] E. Tournefier,[35] A. Trapananti,[189,82] R. Travaglini,[78] F. Travasso,[189,82] G. Traylor,[68] L. Traylor,[57] M. Trevor,[136] M. C. Tringali,[67] A. Tripathee,[157] G. Troian,[187,188] A. Trovato,[187,188] L. Trozzo,[5] R. J. Trudeau,[11] T. Tsang,[331] S. Tsuchida,[332] K. Tsuji,[52] L. Tsukada,[224] A. Tuci,[50] M. Turconi,[118] C. Turski,[96] H. Ubach,[133,134] A. S. Ubhi,[131] N. Uchikata,[220] T. Uchiyama,[53] R. P. Udall,[119] T. Uehara,[333] V. Undheim,[296] V. Upadhyaya,[144] L. E. Uronen,[229] T. Ushiba,[53] M. Vacatello,[87,88] H. Vahlbruch,[9,10] G. Vajente,[11] J. Valencia,[83] M. Valentini,[127,37] E. Vallejo-Pagès,[165] S. A. Vallejo-Peña,[312] S. Vallero,[64] M. van Dael,[37,334] E. Van den Bossche,[195] J. F. J. van den Brand,[36,127,37] C. Van Den Broeck,[76,37] M. van der Kolk,[127] M. van der Sluys,[76,37] A. Van de Walle,[42] J. van Dongen,[37] K. Vandra,[104] M. VanDyke,[126] H. van Haevermaet,[23] J. V. van Heijningen,[37] P. Van Hove,[70] J. Vanier,[274] J. Vanosky,[3] N. van Remortel,[23] M. Vardaro,[36,37] A. F. Vargas,[132] V. Varma,[144] A. Vecchio,[131] G. Vedovato,[94] J. Veitch,[90] P. J. Veitch,[123] S. Venikoudis,[15] P. Verdier,[60] M. Vereecken,[96] D. Verkindt,[35] B. Verma,[144] S. Verma,[115] Y. Verma,[106] S. M. Vermeulen,[11]

F. Vetrano,[65] A. Veutro,[38, 39] A. Viceré,[65, 66] S. Vidyant,[84] A. D. Viets,[323] A. Vijaykumar,[199] A. Vilkha,[197] N. Villanueva Espinosa,[145] E. T. Vincent,[61] J.-Y. Vinet,[118] S. Viret,[60] S. Vitale,[34] A. Vives,[120] L. Vizmeg,[181] B. Vizzone,[61] H. Vocca,[81, 82] D. Voigt,[27] E. R. G. von Reis,[3] J. S. A. von Wrangel,[9, 10] W. E. Vossius,[247] L. Vujeva,[148] S. P. Vyatchanin,[113] J. Wack,[11] L. E. Wade,[108] M. Wade,[108] K. J. Wagner,[197] L. Wallace,[11] R.-Z. Wan,[335] H. Wang,[245] P. Wang,[149] W. H. Wang,[172] Y. F. Wang,[1] Z. Wang,[152] R. L. Ward,[69] J. Warner,[3] M. Was,[35] T. Washimi,[25] N. Y. Washington,[11] D. Watarai,[44] B. Weaver,[3] S. A. Webster,[90] N. L. Weickhardt,[27] M. Weinert,[9, 10] A. J. Weinstein,[11] R. Weiss,[34, †] L. Wen,[7] K. Wette,[69] C. Wheeler,[68] J. T. Whelan,[197] B. F. Whiting,[49] E. G. Wickens,[77] D. Wilken,[9, 10] B. M. Williams,[126] D. Williams,[90] M. J. Williams,[77] N. S. Williams,[1] J. L. Willis,[11] B. Willke,[9, 10] M. Wils,[98] L. Wimmer,[220] C. W. Winborn,[109] A. Wingfield,[122] J. Winterflood,[7] C. C. Wipf,[11] G. Woan,[90] N. E. Wolfe,[34] H. T. Wong,[150] I. C. F. Wong,[98] T. Wouters,[76, 37] J. L. Wright,[3] M. Wright,[76] B. Wu,[84] C. Wu,[149] D. S. Wu,[9, 10] H. Wu,[149] K. Wu,[126] Z. Wu,[103] E. Wuchner,[57] D. M. Wysocki,[86] V. A. Xu,[33] Y. Xu,[83] N. Yadav,[64] H. Yamamoto,[11] K. Yamamoto,[160] T. S. Yamamoto,[44] T. Yamamoto,[53] R. Yamazaki,[213] T. Yan,[131] H. Yang,[289] K. Z. Yang,[18] Y. Yang,[161] Z. Yarbrough,[12] J. Yébana Carrilero,[83] A. B. Yelikar,[54] X. Yin,[34] J. Yokoyama,[336, 44, 43] T. Yokozawa,[53] M. Yoshihara,[52] S. Yuan,[7] H. Yuzurihara,[53] M. Zanatta,[79] M. Zanolin,[50] M. Zeeshan,[197] T. Zelenova,[67] J.-P. Zendri,[94] M. Zeoli,[15] M. Zerrad,[40] M. Zevin,[99] H. Zhang,[152] J. Zhang,[15] L. Zhang,[11] N. Zhang,[61] R. Zhang,[102] T. Zhang,[131] C. Zhao,[7] J. Zhao,[337] Yue Zhao,[338] Yuhang Zhao,[20] L.-M. Zheng,[32] Y. Zheng,[109] L. Zhizhong,[82] H. Zhong,[18] H. Zhou,[84] H. O. Zhu,[7] X.-J. Zhu,[337] Z.-H. Zhu,[337, 335] Z. Zhu,[197] D. Z. Zieba,[90] A. B. Zimmerman,[155] L. Zimmermann,[60] and M. E. Zucker[34, 11]

(The LIGO Scientific Collaboration, the Virgo Collaboration, and the KAGRA Collaboration)

[1] *Max Planck Institute for Gravitational Physics (Albert Einstein Institute), D-14476 Potsdam, Germany*
[2] *Department of Physics, Graduate School of Science, Osaka Metropolitan University, 3-3-138 Sugimoto-cho, Sumiyoshi-ku, Osaka City, Osaka 558-8585, Japan*
[3] *LIGO Hanford Observatory, Richland, WA 99352, USA*
[4] *Dipartimento di Fisica "E.R. Caianiello", Università di Salerno, I-84084 Fisciano, Salerno, Italy*
[5] *INFN, Sezione di Napoli, I-80126 Napoli, Italy*
[6] *University of Warwick, Coventry CV4 7AL, United Kingdom*
[7] *OzGrav, University of Western Australia, Crawley, Western Australia 6009, Australia*
[8] *The Pennsylvania State University, University Park, PA 16802, USA*
[9] *Max Planck Institute for Gravitational Physics (Albert Einstein Institute), D-30167 Hannover, Germany*
[10] *Leibniz Universität Hannover, D-30167 Hannover, Germany*
[11] *LIGO Laboratory, California Institute of Technology, Pasadena, CA 91125, USA*
[12] *Louisiana State University, Baton Rouge, LA 70803, USA*
[13] *Tata Institute of Fundamental Research, Mumbai 400005, India*
[14] *Centre de Physique Théorique, Aix-Marseille Université, Campus de Luminy, 163 Av. de Luminy, 13009 Marseille, France*
[15] *Université catholique de Louvain, B-1348 Louvain-la-Neuve, Belgium*
[16] *Queen Mary University of London, London E1 4NS, United Kingdom*
[17] *University of California, Davis, Davis, CA 95616, USA*
[18] *University of Minnesota, Minneapolis, MN 55455, USA*
[19] *Instituto Nacional de Pesquisas Espaciais, 12227-010 São José dos Campos, São Paulo, Brazil*
[20] *Université Paris Cité, CNRS, Astroparticule et Cosmologie, F-75013 Paris, France*
[21] *Università di Roma Tor Vergata, I-00133 Roma, Italy*
[22] *INFN, Sezione di Roma Tor Vergata, I-00133 Roma, Italy*
[23] *Universiteit Antwerpen, 2000 Antwerpen, Belgium*
[24] *International Centre for Theoretical Sciences, Tata Institute of Fundamental Research, Bengaluru 560089, India*
[25] *Gravitational Wave Science Project, National Astronomical Observatory of Japan, 2-21-1 Osawa, Mitaka City, Tokyo 181-8588, Japan*
[26] *Advanced Technology Center, National Astronomical Observatory of Japan, 2-21-1 Osawa, Mitaka City, Tokyo 181-8588, Japan*
[27] *Universität Hamburg, D-22761 Hamburg, Germany*
[28] *INFN, Sezione di Genova, I-16146 Genova, Italy*
[29] *Dipartimento di Fisica, Università degli Studi di Genova, I-16146 Genova, Italy*
[30] *Research Center for Space Science, Advanced Research Laboratories, Tokyo City University, 3-3-1 Ushikubo-Nishi, Tsuzuki-Ku, Yokohama, Kanagawa 224-8551, Japan*
[31] *Università di Napoli "Federico II", I-80126 Napoli, Italy*
[32] *Cardiff University, Cardiff CF24 3AA, United Kingdom*
[33] *University of California, Berkeley, CA 94720, USA*

[34] LIGO Laboratory, Massachusetts Institute of Technology, Cambridge, MA 02139, USA
[35] Univ. Savoie Mont Blanc, CNRS, Laboratoire d'Annecy de Physique des Particules - IN2P3, F-74000 Annecy, France
[36] Maastricht University, 6200 MD Maastricht, Netherlands
[37] Nikhef, 1098 XG Amsterdam, Netherlands
[38] INFN, Sezione di Roma, I-00185 Roma, Italy
[39] Università di Roma "La Sapienza", I-00185 Roma, Italy
[40] Aix Marseille Univ, CNRS, Centrale Med, Institut Fresnel, F-13013 Marseille, France
[41] OzGrav, School of Physics & Astronomy, Monash University, Clayton 3800, Victoria, Australia
[42] Université Paris-Saclay, CNRS/IN2P3, IJCLab, 91405 Orsay, France
[43] Department of Physics, The University of Tokyo,
7-3-1 Hongo, Bunkyo-ku, Tokyo 113-0033, Japan
[44] Research Center for the Early Universe (RESCEU),
The University of Tokyo, 7-3-1 Hongo, Bunkyo-ku, Tokyo 113-0033, Japan
[45] University of Zurich, Winterthurerstrasse 190, 8057 Zurich, Switzerland
[46] University of California, Riverside, Riverside, CA 92521, USA
[47] Gran Sasso Science Institute (GSSI), I-67100 L'Aquila, Italy
[48] INFN, Laboratori Nazionali del Gran Sasso, I-67100 Assergi, Italy
[49] University of Florida, Gainesville, FL 32611, USA
[50] Embry-Riddle Aeronautical University, Prescott, AZ 86301, USA
[51] Tecnologico de Monterrey, Escuela de Ingeniería y Ciencias, 64849 Monterrey, Nuevo León, Mexico
[52] Nagoya University, Nagoya, 464-8601, Japan
[53] KAGRA Observatory, Institute for Cosmic Ray Research, The University of Tokyo,
238 Higashi-Mozumi, Kamioka-cho, Hida City, Gifu 506-1205, Japan
[54] Vanderbilt University, Nashville, TN 37235, USA
[55] University of Washington, Seattle, WA 98195, USA
[56] Earthquake Research Institute, The University of Tokyo,
1-1-1 Yayoi, Bunkyo-ku, Tokyo 113-0032, Japan
[57] California State University Fullerton, Fullerton, CA 92831, USA
[58] Department of Applied Physics, Graduate School of Engineering,
The University of Tokyo, 7-3-1 Hongo, Bunkyo-ku, Tokyo 113-8656, Japan
[59] SUPA, University of Strathclyde, Glasgow G1 1XQ, United Kingdom
[60] Université Claude Bernard Lyon 1, CNRS, IP2I Lyon / IN2P3, UMR 5822, F-69622 Villeurbanne, France
[61] Georgia Institute of Technology, Atlanta, GA 30332, USA
[62] Royal Holloway, University of London, London TW20 0EX, United Kingdom
[63] Department of Astronomical Science, The Graduate University for Advanced Studies (SOKENDAI),
2-21-1 Osawa, Mitaka City, Tokyo 181-8588, Japan
[64] INFN Sezione di Torino, I-10125 Torino, Italy
[65] Università degli Studi di Urbino "Carlo Bo", I-61029 Urbino, Italy
[66] INFN, Sezione di Firenze, I-50019 Sesto Fiorentino, Firenze, Italy
[67] European Gravitational Observatory (EGO), I-56021 Cascina, Pisa, Italy
[68] LIGO Livingston Observatory, Livingston, LA 70754, USA
[69] OzGrav, Australian National University, Canberra, Australian Capital Territory 0200, Australia
[70] Université de Strasbourg, CNRS, IPHC UMR 7178, F-67000 Strasbourg, France
[71] King's College London, University of London, London WC2R 2LS, United Kingdom
[72] Korea Institute of Science and Technology Information, Daejeon 34141, Republic of Korea
[73] Département de Physique Nucléaire et Corpusculaire,
Université de Genève, 24 quai E. Ansermet, CH-1211 Geneva, Switzerland
[74] Gravitational Wave Science Center, UniGe, -, Switzerland
[75] International College, The University of Osaka,
1-1 Machikaneyama-cho, Toyonaka City, Osaka 560-0043, Japan
[76] Institute for Gravitational and Subatomic Physics (GRASP),
Utrecht University, 3584 CC Utrecht, Netherlands
[77] University of Portsmouth, Portsmouth, PO1 3FX, United Kingdom
[78] Istituto Nazionale Di Fisica Nucleare - Sezione di Bologna,
viale Carlo Berti Pichat 6/2 - 40127 Bologna, Italy
[79] Università di Trento, Dipartimento di Fisica, I-38123 Povo, Trento, Italy
[80] INFN, Trento Institute for Fundamental Physics and Applications, I-38123 Povo, Trento, Italy
[81] Università di Perugia, I-06123 Perugia, Italy
[82] INFN, Sezione di Perugia, I-06123 Perugia, Italy
[83] IAC3–IEEC, Universitat de les Illes Balears, E-07122 Palma de Mallorca, Spain
[84] Syracuse University, Syracuse, NY 13244, USA
[85] Inter-University Centre for Astronomy and Astrophysics, Pune 411007, India
[86] University of Wisconsin-Milwaukee, Milwaukee, WI 53201, USA
[87] INFN, Sezione di Pisa, I-56127 Pisa, Italy

[88]Università di Pisa, I-56127 Pisa, Italy
[89]Dipartimento di Medicina, Chirurgia e Odontoiatria "Scuola Medica Salernitana", Università di Salerno, I-84081 Baronissi, Salerno, Italy
[90]IGR, University of Glasgow, Glasgow G12 8QQ, United Kingdom
[91]HUN-REN Wigner Research Centre for Physics, H-1121 Budapest, Hungary
[92]Stanford University, Stanford, CA 94305, USA
[93]Università di Padova, Dipartimento di Fisica e Astronomia, I-35131 Padova, Italy
[94]INFN, Sezione di Padova, I-35131 Padova, Italy
[95]Institute for Plasma Research, Bhat, Gandhinagar 382428, India
[96]Universiteit Gent, B-9000 Gent, Belgium
[97]Nicolaus Copernicus Astronomical Center, Polish Academy of Sciences, 00-716, Warsaw, Poland
[98]Katholieke Universiteit Leuven, Oude Markt 13, 3000 Leuven, Belgium
[99]Northwestern University, Evanston, IL 60208, USA
[100]Centro de Investigaciones Energéticas Medioambientales y Tecnológicas, Avda. Complutense 40, 28040, Madrid, Spain
[101]Aix-Marseille Université, Université de Toulon, CNRS, CPT, Marseille, France
[102]Northeastern University, Boston, MA 02115, USA
[103]Laboratoire des 2 infinis - Toulouse, Université de Toulouse, CNRS/IN2P3, Toulouse, France, Toulouse, France
[104]Villanova University, Villanova, PA 19085, USA
[105]Federal University of Rio Grande do Norte, Campus Universitário - Lagoa Nova, Natal - RN, 59078-970, Brazil
[106]RRCAT, Indore, Madhya Pradesh 452013, India
[107]University of Maryland, Baltimore County, Baltimore, MD 21250, USA
[108]Kenyon College, Gambier, OH 43022, USA
[109]Missouri University of Science and Technology, Rolla, MO 65409, USA
[110]Indian Institute of Technology Madras, Chennai 600036, India
[111]Indian Institute of Technology Bombay, Powai, Mumbai 400 076, India
[112]Università di Siena, Dipartimento di Scienze Fisiche, della Terra e dell'Ambiente, I-53100 Siena, Italy
[113]Lomonosov Moscow State University, Moscow 119991, Russia
[114]Center for Theoretical Physics, Polish Academy of Sciences, 02-668, Warsaw, Poland
[115]Université libre de Bruxelles, 1050 Bruxelles, Belgium
[116]Bar-Ilan University, Ramat Gan, 5290002, Israel
[117]Princeton University, Princeton, NJ 08544 USA
[118]Université Côte d'Azur, Observatoire de la Côte d'Azur, CNRS, Artemis, F-06304 Nice, France
[119]University of British Columbia, Vancouver, BC V6T 1Z4, Canada
[120]University of Oregon, Eugene, OR 97403, USA
[121]Subatech, CNRS/IN2P3 - IMT Atlantique - Nantes Université, 4 rue Alfred Kastler BP 20722 44307 Nantes CÉDEX 03, France
[122]Christopher Newport University, Newport News, VA 23606, USA
[123]OzGrav, University of Adelaide, Adelaide, South Australia 5005, Australia
[124]Centre national de la recherche scientifique, 75016 Paris, France
[125]DIFA- Alma Mater Studiorum Università di Bologna, Via Zamboni, 33 - 40126 Bologna, Italy
[126]Washington State University, Pullman, WA 99164, USA
[127]Department of Physics and Astronomy, Vrije Universiteit Amsterdam, 1081 HV Amsterdam, Netherlands
[128]Cornell University, Ithaca, NY 14850, USA
[129]University of Rhode Island, Kingston, RI 02881, USA
[130]Laboratoire Kastler Brossel, Sorbonne Université, CNRS, ENS-Université PSL, Collège de France, F-75005 Paris, France
[131]University of Birmingham, Birmingham B15 2TT, United Kingdom
[132]OzGrav, University of Melbourne, Parkville, Victoria 3010, Australia
[133]Institut de Ciències del Cosmos (ICCUB), Universitat de Barcelona (UB), c. Martí i Franquès, 1, 08028 Barcelona, Spain
[134]Departament de Física Quàntica i Astrofísica (FQA), Universitat de Barcelona (UB), c. Martí i Franqués, 1, 08028 Barcelona, Spain
[135]Astronomical Observatory, University of Warsaw, 00-478 Warsaw, Poland
[136]University of Maryland, College Park, MD 20742, USA
[137]Università degli Studi di Milano-Bicocca, I-20126 Milano, Italy
[138]INFN, Sezione di Milano-Bicocca, I-20126 Milano, Italy
[139]IGFAE, Universidade de Santiago de Compostela, E-15782 Santiago de Compostela, Spain
[140]Williams College, Williamstown, MA 01267 USA
[141]University of Arizona, Tucson, AZ 85721, USA
[142]Faculty of Physics, University of Warsaw, Ludwika Pasteura 5, 02-093 Warszawa, Poland
[143]Istituto di Astrofisica e Planetologia Spaziali di Roma, 00133 Roma, Italy

[144]University of Massachusetts Dartmouth, North Dartmouth, MA 02747, USA
[145]Departamento de Astronomía y Astrofísica, Universitat de València, E-46100 Burjassot, València, Spain
[146]Observatori Astronòmic, Universitat de València, E-46980 Paterna, València, Spain
[147]OzGrav, Swinburne University of Technology, Hawthorn VIC 3122, Australia
[148]Niels Bohr Institute, University of Copenhagen, 2100 Kóbenhavn, Denmark
[149]Department of Physics, National Tsing Hua University, No. 101 Section 2, Kuang-Fu Road, Hsinchu 30013, Taiwan
[150]National Central University, Taoyuan City 320317, Taiwan
[151]OzGrav, Charles Sturt University, Wagga Wagga, New South Wales 2678, Australia
[152]University of Chinese Academy of Sciences / International Centre for Theoretical Physics Asia-Pacific, Beijing 100190, China
[153]Institute of Physics, National Yang Ming Chiao Tung University, 101 Univ. Street, Hsinchu, Taiwan
[154]Kamioka Branch, National Astronomical Observatory of Japan, 238 Higashi-Mozumi, Kamioka-cho, Hida City, Gifu 506-1205, Japan
[155]University of Texas, Austin, TX 78712, USA
[156]CaRT, California Institute of Technology, Pasadena, CA 91125, USA
[157]University of Michigan, Ann Arbor, MI 48109, USA
[158]Dipartimento di Ingegneria Industriale (DIIN), Università di Salerno, I-84084 Fisciano, Salerno, Italy
[159]INFN, Sezione di Napoli, Gruppo Collegato di Salerno, I-80126 Napoli, Italy
[160]Faculty of Science, University of Toyama, 3190 Gofuku, Toyama City, Toyama 930-8555, Japan
[161]School of Physical Science and Technology, ShanghaiTech University, 393 Middle Huaxia Road, Pudong, Shanghai, 201210, China
[162]Carleton College, Northfield, MN 55057, USA
[163]University of Szeged, Dóm tér 9, Szeged 6720, Hungary
[164]St. Thomas University, Miami Gardens, FL 33054, USA
[165]Institut de Física d'Altes Energies (IFAE), The Barcelona Institute of Science and Technology, Campus UAB, E-08193 Bellaterra (Barcelona), Spain
[166]INFN Cagliari, Physics Department, Università degli Studi di Cagliari, Cagliari 09042, Italy
[167]Université Libre de Bruxelles, Brussels 1050, Belgium
[168]INAF, Osservatorio Astronomico di Brera sede di Merate, I-23807 Merate, Lecco, Italy
[169]Departamento de Matemáticas, Universitat de València, E-46100 Burjassot, València, Spain
[170]Montana State University, Bozeman, MT 59717, USA
[171]Johns Hopkins University, Baltimore, MD 21218, USA
[172]The University of Texas Rio Grande Valley, Brownsville, TX 78520, USA
[173]Instituto de Ciências e Tecnologia - Universidade Federal de Alfenas, BR 267 - Rodovia José Aurélio Vilela, nº11.999, Km 533 37715-400 Cidade Universitária - Poços de Caldas - MG - Brasil, Brazil
[174]University of Manitoba, Winnipeg, MB R3T 2N2, Canada
[175]INFN-CNAF - Bologna, Viale Carlo Berti Pichat, 6/2, 40127 Bologna BO, Italy
[176]Colorado State University, Fort Collins, CO 80523, USA
[177]Université de Normandie, ENSICAEN, UNICAEN, CNRS/IN2P3, LPC Caen, F-14000 Caen, France
[178]Laboratoire de Physique Corpusculaire Caen, 6 boulevard du maréchal Juin, F-14050 Caen, France
[179]The University of Sheffield, Sheffield S10 2TN, United Kingdom
[180]Université Claude Bernard Lyon 1, CNRS, Laboratoire des Matériaux Avancés (LMA), IP2I Lyon / IN2P3, UMR 5822, F-69622 Villeurbanne, France
[181]Western Washington University, Bellingham, WA 98225, USA
[182]Università di Firenze, Sesto Fiorentino I-50019, Italy
[183]Università di Parma, I-43124 Parma, Italy
[184]INFN, Sezione di Milano Bicocca, Gruppo Collegato di Parma, I-43124 Parma, Italy
[185]Bard College, Annandale-On-Hudson, NY 12504, USA
[186]Marquette University, Milwaukee, WI 53233, USA
[187]Dipartimento di Fisica, Università di Trieste, I-34127 Trieste, Italy
[188]INFN, Sezione di Trieste, I-34127 Trieste, Italy
[189]Università di Camerino, I-62032 Camerino, Italy
[190]Scuola Normale Superiore, I-56126 Pisa, Italy
[191]Corps des Mines, Mines Paris, Université PSL, 60 Bd Saint-Michel, 75272 Paris, France
[192]Université Côte d'Azur, Observatoire de la Côte d'Azur, CNRS, Lagrange, F-06304 Nice, France
[193]National Center for Nuclear Research, 05-400 Świerk-Otwock, Poland
[194]Università degli Studi di Sassari, I-07100 Sassari, Italy
[195]Vrije Universiteit Brussel, 1050 Brussel, Belgium
[196]Trinity College, Hartford, CT 06106, USA
[197]Rochester Institute of Technology, Rochester, NY 14623, USA

[198] Université de Liège, B-4000 Liège, Belgium
[199] Canadian Institute for Theoretical Astrophysics, University of Toronto, Toronto, ON M5S 3H8, Canada
[200] Perimeter Institute, Waterloo, ON N2L 2Y5, Canada
[201] Stony Brook University, Stony Brook, NY 11794, USA
[202] Center for Computational Astrophysics, Flatiron Institute, New York, NY 10010, USA
[203] Montclair State University, Montclair, NJ 07043, USA
[204] HUN-REN Institute for Nuclear Research, H-4026 Debrecen, Hungary
[205] Centro de Física das Universidades do Minho e do Porto, Universidade do Minho, PT-4710-057 Braga, Portugal
[206] Aix Marseille Univ, CNRS/IN2P3, CPPM, Marseille, France
[207] Dipartimento di Ingegneria, Università della Basilicata, I-85100 Potenza, Italy
[208] SUPA, University of the West of Scotland, Paisley PA1 2BE, United Kingdom
[209] Barry University, Miami Shores, FL 33168, USA
[210] Department of Astronomy, University of Geneva, Chemin Pegasi 51, 1290 Versoix, Switzerland
[211] Centro de Astrofísica e Gravitação, Departamento de Física, Instituto Superior Técnico - IST, Universidade de Lisboa - UL, Av. Rovisco Pais 1, 1049-001 Lisboa, Portugal
[212] Eötvös University, Budapest 1117, Hungary
[213] Department of Physical Sciences, Aoyama Gakuin University, 5-10-1 Fuchinobe, Sagamihara City, Kanagawa 252-5258, Japan
[214] University of Sannio at Benevento, I-82100 Benevento, Italy and INFN, Sezione di Napoli, I-80100 Napoli, Italy
[215] California State University, Los Angeles, Los Angeles, CA 90032, USA
[216] Instituto de Fisica Teorica UAM-CSIC, Universidad Autonoma de Madrid, 28049 Madrid, Spain
[217] Istituto Nazionale di Astrofisica - Osservatorio di Roma, Viale del Parco Mellini 84 - 00136 Roma, Italy
[218] Laboratoire d'Acoustique de l'Université du Mans, UMR CNRS 6613, F-72085 Le Mans, France
[219] University of Southampton, Southampton SO17 1BJ, United Kingdom
[220] KAGRA Observatory, Institute for Cosmic Ray Research, The University of Tokyo, 5-1-5 Kashiwa-no-Ha, Kashiwa City, Chiba 277-8582, Japan
[221] Faculty of Physics, University of Białystok, 15-245 Białystok, Poland
[222] University of Nottingham NG7 2RD, UK
[223] Dipartimento di Ingegneria Industriale, Elettronica e Meccanica, Università degli Studi Roma Tre, I-00146 Roma, Italy
[224] University of Nevada, Las Vegas, Las Vegas, NV 89154, USA
[225] University of Chicago, Chicago, IL 60637, USA
[226] The University of Mississippi, University, MS 38677, USA
[227] Institute of Physics, Academia Sinica, 128 Sec. 2, Academia Rd., Nankang, Taipei 11529, Taiwan
[228] Shanghai Astronomical Observatory, Chinese Academy of Sciences, 80 Nandan Road, Shanghai 200030, China
[229] The Chinese University of Hong Kong, Shatin, NT, Hong Kong
[230] Nirula Institute of Technology, Kolkata, West Bengal 700109, India
[231] American University, Washington, DC 20016, USA
[232] Aix Marseille Université, Jardin du Pharo, 58 Boulevard Charles Livon, 13007 Marseille, France
[233] Dipartimento di Fisica, Università degli studi di Milano, Via Celoria 16, I-20133, Milano, Italy
[234] INFN, sezione di Milano, Via Celoria 16, I-20133, Milano, Italy
[235] Department of Applied Physics, Fukuoka University, 8-19-1 Nanakuma, Jonan, Fukuoka City, Fukuoka 814-0180, Japan
[236] University of Cambridge, Cambridge CB2 1TN, United Kingdom
[237] University of Lancaster, Lancaster LA1 4YW, United Kingdom
[238] College of Industrial Technology, Nihon University, 1-2-1 Izumi, Narashino City, Chiba 275-8575, Japan
[239] Saha Institute of Nuclear Physics, Bidhannagar, West Bengal 700064, India
[240] Institute of Photonics Technologies, National Tsing Hua University, No. 101 Section 2, Kuang-Fu Road, Hsinchu 30013, Taiwan
[241] Department of Physics, Tamkang University, No. 151, Yingzhuan Rd., Danshui Dist., New Taipei City 25137, Taiwan
[242] Department of Electrophysics, National Yang Ming Chiao Tung University, 101 Univ. Street, Hsinchu, Taiwan
[243] Rutherford Appleton Laboratory, Didcot OX11 0DE, United Kingdom
[244] Department of Astronomy and Space Science, Chungnam National University, 9 Daehak-ro, Yuseong-gu, Daejeon 34134, Republic of Korea
[245] Graduate School of Science, Institute of Science Tokyo, 2-12-1 Ookayama, Meguro-ku, Tokyo 152-8551, Japan
[246] Columbia University, New York, NY 10027, USA
[247] Helmut Schmidt University, D-22043 Hamburg, Germany

[248] Nambu Yoichiro Institute of Theoretical and Experimental Physics (NITEP), Osaka Metropolitan University, 3-3-138 Sugimoto-cho, Sumiyoshi-ku, Osaka City, Osaka 558-8585, Japan
[249] Directorate of Construction, Services & Estate Management, Mumbai 400094, India
[250] Royal Observatory of Belgium, Avenue Circulaire, 3, 1180 Uccle, Belgium
[251] Observatoire Astronomique de Strasbourg, Université de Strasbourg, CNRS, 11 rue de l'Université, 67000 Strasbourg, France
[252] National Astronomical Observatories, Chinese Academy of Sciences, 20A Datun Road, Chaoyang District, Beijing, China
[253] School of Astronomy and Space Science, University of Chinese Academy of Sciences, 20A Datun Road, Chaoyang District, Beijing, China
[254] Sungkyunkwan University, Seoul 03063, Republic of Korea
[255] Department of Physics, Ulsan National Institute of Science and Technology (UNIST), 50 UNIST-gil, Ulju-gun, Ulsan 44919, Republic of Korea
[256] Chung-Ang University, Seoul 06974, Republic of Korea
[257] Vrije Universiteit Amsterdam, 1081 HV, Amsterdam, Netherlands
[258] University of Washington Bothell, Bothell, WA 98011, USA
[259] Université Paris-Saclay, Université Paris Cité, CEA, CNRS, AIM, 91191, Gif-sur-Yvette, France
[260] Ewha Womans University, Seoul 03760, Republic of Korea
[261] Department of Astronomy, Yonsei University, 50 Yonsei-Ro, Seodaemun-Gu, Seoul 03722, Republic of Korea
[262] National Institute for Mathematical Sciences, Daejeon 34047, Republic of Korea
[263] Korea Astronomy and Space Science Institute, Daejeon 34055, Republic of Korea
[264] Division of Science, National Astronomical Observatory of Japan, 2-21-1 Osawa, Mitaka City, Tokyo 181-8588, Japan
[265] Department of Physics, Aristotle University of Thessaloniki, 54124 Thessaloniki, Greece
[266] National Tsing Hua University, Hsinchu City 30013, Taiwan
[267] Technical University of Braunschweig, D-38106 Braunschweig, Germany
[268] Institute of Mathematics, Polish Academy of Sciences, 00656 Warsaw, Poland
[269] Astronomical Observatory, Jagiellonian University, 31-007 Cracow, Poland
[270] Department of Physics and Helsinki Institute of Physics, University of Helsinki, Gustaf Hallstromin katu 2,, FI-00014, Finland
[271] Instituto de Fisica Teorica UAM-CSIC, Universidad Autonoma de Madrid, 28049 Madrid, Spain
[272] Department of Physics, Nagoya University, ES building, Furocho, Chikusa-ku, Nagoya, Aichi 464-8602, Japan
[273] Centre de Calcul IN2P3, 21 avenue Pierre de Coubertin, Campus de la Doua, 69100 Villeurbanne, France
[274] Université de Montréal/Polytechnique, Montreal, Quebec H3T 1J4, Canada
[275] Università degli Studi di Cagliari, Via Università 40, 09124 Cagliari, Italy
[276] Department of Computer Simulation, Inje University, 197 Inje-ro, Gimhae, Gyeongsangnam-do 50834, Republic of Korea
[277] Korea Astronomy and Space Science Institute (KASI), 776 Daedeokdae-ro, Yuseong-gu, Daejeon 34055, Republic of Korea
[278] NAVIER, École des Ponts, Univ Gustave Eiffel, CNRS, Marne-la-Vallée, France
[279] Gravitational Wave Science Project, National Astronomical Observatory of Japan (NAOJ), Mitaka City, Tokyo 181-8588, Japan
[280] Department of Physics, National Cheng Kung University, No.1, University Road, Tainan City 701, Taiwan
[281] National Center for High-performance Computing, National Institutes of Applied Research, No. 7, R&D 6th Rd., Hsinchu Science Park, Hsinchu City 30076, Taiwan
[282] Institute of Astronomy, National Tsing Hua University, No. 101 Section 2, Kuang-Fu Road, Hsinchu 30013, Taiwan
[283] Institució Catalana de Recerca i Estudis Avançats, E-08010 Barcelona, Spain
[284] Institut de Física d'Altes Energies, E-08193 Barcelona, Spain
[285] Institut fuer Theoretische Astrophysik, Zentrum fuer Astronomie Heidelberg, Universitaet Heidelberg, Albert Ueberle Str. 2, 69120 Heidelberg, Germany
[286] Institucio Catalana de Recerca i Estudis Avançats (ICREA), Passeig de Lluís Companys, 23, 08010 Barcelona, Spain
[287] Université de Lyon, Université Claude Bernard Lyon 1, CNRS, Institut Lumière Matière, F-69622 Villeurbanne, France
[288] Universidade Estadual Paulista, R. Dr. José Barbosa de Barros, 1780 - Jardim Paraiso, Botucatu - SP, 18610-307, Brazil

[289] Tsinghua University, Beijing 100084, China
[290] Departament de Física, Universitat de les Illes Balears,
IAC3 –IEEC, Crta. Valldemossa km 7.5, E-07122 Palma, Spain
[291] Universidad de Guadalajara, 44430 Guadalajara, Jalisco, Mexico
[292] Institut des Hautes Etudes Scientifiques, F-91440 Bures-sur-Yvette, France
[293] Faculty of Law, Ryukoku University, 67 Fukakusa Tsukamoto-cho,
Fushimi-ku, Kyoto City, Kyoto 612-8577, Japan
[294] Indian Institute of Science Education and Research, Kolkata, Mohanpur, West Bengal 741252, India
[295] Phenikaa University, Nguyen Trac Street, Duong Noi, Hanoi, Vietnam
[296] University of Stavanger, 4021 Stavanger, Norway
[297] Department of Astronomy, The University of Tokyo,
7-3-1 Hongo, Bunkyo-ku, Tokyo 113-0033, Japan
[298] Physics Program, Graduate School of Advanced Science and Engineering,
Hiroshima University, 1-3-1 Kagamiyama, Higashihiroshima City, Hiroshima 739-8526, Japan
[299] GRAPPA, Anton Pannekoek Institute for Astronomy and Institute for High-Energy Physics,
University of Amsterdam, 1098 XH Amsterdam, Netherlands
[300] University College London, London WC1E 6BT, United Kingdom
[301] Observatoire de Paris, 75014 Paris, France
[302] Instituto Tecnológico de Aeronáutica, Praça Marechal Eduardo Gomes,
50 - Vila das Acacias, São José dos Campos - SP, 12228-900, Brazil
[303] Graduate School of Science and Technology, Niigata University,
8050 Ikarashi-2-no-cho, Nishi-ku, Niigata City, Niigata 950-2181, Japan
[304] Niigata Study Center, The Open University of Japan, 754 Ichibancho,
Asahimachi-dori, Chuo-ku, Niigata City, Niigata 951-8122, Japan
[305] Consiglio Nazionale delle Ricerche - Istituto dei Sistemi Complessi, I-00185 Roma, Italy
[306] Hobart and William Smith Colleges, Geneva, NY 14456, USA
[307] Dipartimento di Ingegneria, Università del Sannio, I-82100 Benevento, Italy
[308] Institut d'Astrophysique de Paris, Sorbonne Université, CNRS, UMR 7095, 75014 Paris, France
[309] Museo Storico della Fisica e Centro Studi e Ricerche "Enrico Fermi", I-00184 Roma, Italy
[310] Kennesaw State University, Kennesaw, GA 30144, USA
[311] Government Victoria College, Palakkad, Kerala 678001, India
[312] Universidad de Antioquia, Medellín, Colombia
[313] Departamento de Física - ETSIDI, Universidad Politécnica de Madrid, 28012 Madrid, Spain
[314] Ariel University, Ramat HaGolan St 65, Ari'el, Israel
[315] Department of Electronic Control Engineering,
National Institute of Technology, Nagaoka College,
888 Nishikatakai, Nagaoka City, Niigata 940-8532, Japan
[316] Dipartimento di Fisica e Scienze della Terra, Università Degli Studi di Ferrara, Via Saragat, 1, 44121 Ferrara FE, Italy
[317] Faculty of Science, Toho University, 2-2-1 Miyama, Funabashi City, Chiba 274-8510, Japan
[318] Seoul National University, Seoul 08826, Republic of Korea
[319] Kavli Institute for Astronomy and Astrophysics, Peking University,
Yiheyuan Road 5, Haidian District, Beijing 100871, China
[320] Faculty of Information Science and Technology, Osaka Institute of Technology,
1-79-1 Kitayama, Hirakata City, Osaka 573-0196, Japan
[321] NASA Goddard Space Flight Center, Greenbelt, MD 20771, USA
[322] Faculty of Science and Technology, Kochi University,
2-5-1 Akebono-cho, Kochi-shi, Kochi 780-8520, Japan
[323] Concordia University Wisconsin, Mequon, WI 53097, USA
[324] Scuola Internazionale Superiore di Studi Avanzati, Via Bonomea, 265, I-34136, Trieste TS, Italy
[325] Laboratoire de Physique de l'ENS, Université Paris Cité, Ecole Normale Supérieure,
Université PSL, Sorbonne Université, CNRS, 75005 Paris, France
[326] The Hakubi Center for Advanced Research, Kyoto University,
Yoshida-honmachi, Sakyou-ku, Kyoto City, Kyoto 606-8501, Japan
[327] Department of Physics, Kyoto University, Kita-Shirakawa Oiwake-cho, Sakyou-ku, Kyoto City, Kyoto 606-8502, Japan
[328] Yukawa Institute for Theoretical Physics (YITP), Kyoto University,
Kita-Shirakawa Oiwake-cho, Sakyou-ku, Kyoto City, Kyoto 606-8502, Japan
[329] Chennai Mathematical Institute, Chennai 603103, India
[330] University of Catania, Department of Physics and Astronomy, Via S. Sofia, 64, 95123 Catania CT, Italy
[331] Southeastern Louisiana University, Hammond, LA 70402, USA
[332] National Institute of Technology, Fukui College, Geshi-cho, Sabae-shi, Fukui 916-8507, Japan
[333] Department of Communications Engineering, National Defense Academy of Japan,
1-10-20 Hashirimizu, Yokosuka City, Kanagawa 239-8686, Japan
[334] Eindhoven University of Technology, 5600 MB Eindhoven, Netherlands

[335] School of Physics and Technology, Wuhan University, Bayi Road 299, Wuchang District, Wuhan, Hubei, 430072, China
[336] Kavli Institute for the Physics and Mathematics of the Universe (Kavli IPMU), WPI, The University of Tokyo, 5-1-5 Kashiwa-no-Ha, Kashiwa City, Chiba 277-8583, Japan
[337] Department of Astronomy, Beijing Normal University, Xinjiekouwai Street 19, Haidian District, Beijing 100875, China
[338] Hong Kong University of Science and Technology, Clear Water Bay, HK, Hong Kong

We report results from a search for an isotropic stochastic gravitational-wave background using data collected by the LIGO–Virgo–KAGRA Collaboration. The analysis uses data from the first observing run through April 1, 2025, during the fourth observing run. New frequency-domain cuts are implemented to address a class of non-stationary spectral noise features that were not effectively identified and mitigated by existing data-quality checks in past analyses. Consequently, previously analyzed data from the fourth observing run are re-processed with the updated cuts. We find no evidence for a stochastic background signal and place upper limits on the gravitational-wave energy density. In particular, for a background following a power law with spectral index 2/3 as predicted by inspiralling compact binaries, we find $\Omega_{\rm GW}(25\,{\rm Hz}) \leq 2.0 \times 10^{-9}$, while scale-invariant backgrounds are constrained to $\Omega_{\rm GW}(25\,{\rm Hz}) \leq 2.8 \times 10^{-9}$, both at the 95% credible level for a log-uniform prior on $\Omega_{\rm GW}$. Relative to the constraints from previous data recomputed with the new frequency-domain cuts, these limits improve by a factor of 1.4. We also update bounds on alternative gravity scenarios predicting non-standard polarization modes, and we verify that correlated magnetic noise sources remain below the sensitivity of this search. Combining these observational constraints with population models of compact binary coalescences informed by the latest gravitational-wave transient catalog, GWTC-5.0, we predict the amplitude of the compact binary background to be $\Omega_{\rm CBC}(25\,{\rm Hz}) = 6.3^{+5.0}_{-2.2} \times 10^{-10}$ at the 90% credible level.

I. INTRODUCTION

The gravitational-wave background (GWB) is a random superposition of a large number of weak, independent, and unresolved gravitational-wave (GW) signals, of both astrophysical and cosmological origin. Potential astrophysical contributors to the GWB include unresolved compact binary mergers (CBCs) [1–5], core-collapse supernovae [1, 5–9], rotating neutron stars [6, 7, 10–13], and other exotic sources such as superradiance of axion clouds around black holes [14–18]. Possible cosmological sources include cosmic strings [19–32], first-order phase transitions in the early Universe [33–41], primordial black hole binaries [42–45], primordial scalar perturbations [46–51], epochs with a stiff equation of state [52–56], and inflation [57–65].

A detection of the GWB could provide a unique observational window onto the Universe at energy scales and epochs that are inaccessible to electromagnetic observations or terrestrial particle accelerators [66]. In particular, cosmological backgrounds would carry direct information about the physical processes operating in the very early Universe. At the same time, an astrophysical GWB probes the population properties of compact objects at redshifts beyond the reach of individually resolvable GW events [2, 67–70]. The Laser Interferometer Gravitational-wave Observatory (LIGO) [71], Virgo [72], and KAGRA [73] collaborations (LVK Collaboration [74]) have previously placed upper limits on isotropic [75] and anisotropic [76] GWBs as well as on various cosmological models [77] using the data from the first three observing runs (O1, O2, and O3) and the first part of the fourth observing run (O4a).

Given the large number of incoherent and unresolved sources contributing to the GWB, the signal is naturally described within a statistical framework [78–80]. Under the assumption that the individual contributions are independent, the central limit theorem implies that the GWB can be modeled as a Gaussian stochastic process [79] whose strain has zero mean [81], which we further assume to be stationary, isotropic, and unpolarized. Its statistical properties are fully characterized by the two-point correlation function, or equivalently by its energy density spectrum. The optimal estimator is therefore obtained via a cross-correlation analysis between pairs of spatially separated detectors [78–80], exploiting the fact that a stochastic background induces correlated signals across the network. A summary of this formalism is provided in Sec. II of Ref. [75], with comprehensive reviews available in Refs. [78–80, 82].

In this work, we extend previous isotropic GWB searches [75] by incorporating data from the second and early third parts of the LVK Collaboration's fourth observing run (hereafter denoted O4b [83] and O4c1, respectively). We restrict the O4c data set to the period before the scheduled O4c observing break, during which operations were paused from April 1 to June 4, 2025 for maintenance and commissioning work, including the repair of a faulty beam-tube gate valve at LIGO Livingston and other detector improvements intended to reduce risks in the transition from O4 to O5 [84].

We perform a hybrid frequentist-Bayesian cross-correlation analysis [75, 79, 85] implemented in the open-

[*] Deceased, March 2026.
[†] Deceased, August 2025.

source analysis pipeline `pygwb` [86, 87], and update upper limits on the GWB energy density. Our analysis assumes that detector noise is uncorrelated with the GW signal and between different detectors. While the latter assumption is standard in GWB searches [75], we explicitly assess its validity in this work and verify that correlated magnetic noise [88–94] remains negligible.

General relativity (GR) predicts only tensor polarizations, but many alternative theories of gravity allow for additional scalar and vector modes. We therefore extend our isotropic GWB signal model to include tensor, vector, and scalar polarizations and place corresponding upper limits on the amplitude of each component [95, 96].

In the most sensitive frequency band of the current ground-based detector network, the GWB is expected to be dominated by the superposition of unresolved CBCs [97]. Building on the methodology of Ref. [75], we update predictions for the spectrum from binary black holes (BBHs), binary neutron stars (BNSs), and neutron star–black hole (NSBH) coalescences based on the astrophysical distribution of compact binary mergers reported in the recent GWTC-5.0 catalog [98, 99]. We compare such estimates with the latest projections of sensitivity curves for future observing runs [100] and revise previous statements about the detection prospects.

This paper is organized as follows. In Sec. II, we describe the data quality of the additional data included in our analysis. Sec. III presents the main results of our search, including the cross-correlation spectra (Sec. III A), updated upper limits on the GWB (Sec. III B), improved constraints on additional polarization components (Sec. III C), and a joint analysis of magnetic noise and stochastic signals (Sec. III D). Finally, in Sec. IV, we update the predicted amplitude of the compact binary background.

II. DATA QUALITY

In this section, we describe the data quality of the strain data from the LIGO Hanford and LIGO Livingston detectors during O4b and O4c1. These data sets are combined with those from previous observing runs, namely O1–O4a LIGO data together with Virgo O3 data [75, 101–103]. The O4b observing period started at 17:00 UTC on April 10, 2024 and ended at 17:00 UTC on January 28, 2025. Throughout O4b there were two notable breaks during which the interferometers were taken out of observing mode to diagnose and address issues impacting the sensitivity. At LIGO Hanford, operations were interrupted between July 13 and August 24, 2024 due to issues related to the output Faraday isolator. At LIGO Livingston, a separate break occurred between October 11 and October 29, 2024, associated with a fast shutter malfunction. The O4c1 observing period ran without interruption after the end of O4b from 17:00 UTC on January 28, 2025, to 15:00 UTC April 1, 2025. Further details on detector performance and commissioning activities during O4b and O4c1 can be found in Ref. [104]. In the following, we shall refer to the LIGO Hanford detector as LHO and the LIGO Livingston detector as LLO.

The Virgo detector also collected data during O4b and O4c1. However, in the remainder of this work we use only the data from the LHO and LLO detectors during that period. The decision not to include the Virgo data in our analysis is motivated by its marginal contribution to improving the search sensitivity. Quantitatively, we estimate that including Virgo data would lead to improvements in σ_o (Eq. (8) in Ref. [75]) of only 1% during O4b. Virgo data from the third observing run are nevertheless incorporated in our combined analysis. In addition, KAGRA data were not included in this study, as their contribution would be even smaller than that of the Virgo data.

A. Data

The total coincident observing time for the Hanford–Livingston detector baseline from the two periods was 140.99 days, before applying data-quality cuts. For this analysis, we use the calibrated strain data product [83] with low-latency subtractions of sinusoidal calibration lines, 60 Hz power lines [105], and residual noise coupling where available [106]. The data channel is `GDS-CALIB_STRAIN_CLEAN_AR`, and the search is restricted to the frequency range 20–1726 Hz.

B. Time-domain cuts

We apply a series of time-domain data-quality cuts at different stages of the analysis, following the procedures described in Ref. [75]. We summarize in Table I the amount of data remaining after the application of the CAT1 vetoes, which remove data collected while the detectors were operating outside nominal conditions [104], and the final livetime after data preprocessing, including gating, which suppresses periods affected by excess noise by applying an inverse Tukey window to the affected regions of the strain data, effectively setting the corresponding data to zero. The postprocessed data are then subjected to the $\Delta\sigma$ cut, a non-stationarity cut that removes periods during which the square root of the variance varies by more than 20% between neighbouring segments. We highlight that 0.078% of LHO data and 0.068% of LLO data were gated and that 9% of the analyzed segments were discarded following the delta-sigma cut for broadband non-stationarities. These noise artifacts produce excess power distributed over multiple frequency bins, rather than being confined to a single frequency bin of width 1/32 Hz used in the analysis. This leaves a total of 117.05 days of usable data for the analyses presented in this work.

Selection Step	Days
Coincident observing time	140.99
Time after CAT1 vetoes	138.37
Final livetime	117.05

TABLE I. Total duration of coincident data between detectors during O4b and O4c1, together with the amount of data remaining after the application of time-domain data-quality cuts.

C. Frequency-domain cuts

We perform a targeted re-assessment of the frequency domain cuts applied in Ref. [75] to the analysis band 20–1726 Hz and update them for this work. The procedure is motivated by features observed in the cross-spectral density (CSD) and in the individual detector power spectral densities (PSDs), as well as by their impact on the posterior distributions of the parameters of the model adopted to describe the GWB. Specifically, we assume a power-law model of the form

$$\Omega_{\rm GW}(f) = \Omega_{\rm ref}\left(\frac{f}{25\,{\rm Hz}}\right)^{\alpha}, \qquad (1)$$

where $\Omega_{\rm ref}$ is the GWB amplitude at the reference frequency of 25 Hz, and α is the spectral index.

In addition to dedicated investigations of specific spectral features, we implement a procedure to identify frequency bands exhibiting non-stationary behavior throughout the observing period. This approach is based on the temporal variability of the PSD and provides a complementary method to construct our frequency-domain cuts. For each detector, we compute the standard deviation of the PSD normalized by its median value across time segments produced by `pygwb` [86, 87],

$$\mathrm{StdRatio}(f) = \mathrm{std}\left(\frac{\mathrm{PSD}(f)}{\mathrm{median}(\mathrm{PSD}(f))}\right). \qquad (2)$$

The median and standard deviation are computed over all time segments for a given frequency f. We then estimate a smooth local baseline for StdRatio(f) by identifying broadband, peak-like structures - regions that rise well above a running median-filtered baseline - and interpolating linearly across them. This interpolation is used only to construct a baseline representative of the typical variability level, and no features are flagged for removal at this point. The original StdRatio(f) spectrum is divided by this smooth baseline to form a normalized variability spectrum, in which frequencies with excess temporal variability relative to nearby frequencies are enhanced. An empirical threshold of 1.5 is then applied to flag outlier bins, which are subsequently merged into contiguous frequency bands to produce an initial, unvetted list. Each flagged band is vetted by cross-checking against the catalog of known instrumental spectral artifacts [107]. This resulting list, combined with the targeted studies described below, forms the *strict* notch list, which is in turn combined with the baseline notch list of Ref. [75] to produce the final set of frequency-domain cuts applied in this analysis. This procedure provides a complementary view of detector performance, highlighting frequency bands that fluctuate significantly over the course of the observing run, or sidebands of known artifacts such as the power-line harmonics, that are not always apparent in the run-averaged PSDs or coherence spectra used to construct the baseline notch list of Ref. [75].

*a. Updated power-line harmonics (*20–1726 Hz*).* The notches around the 60 Hz power-line harmonics are re-evaluated across the full analysis band. In O4 data, several harmonics exhibited slow frequency wandering and sideband structure, leading to residual contamination outside the nominal narrow notches. These features are consistently identified by the strict procedure described above as regions of excess variability, which support the need for widened notches beyond the nominal harmonic frequencies.

b. Low-frequency region (< 100 Hz*).* Below 100 Hz, which contributes most significantly to the sensitivity for physically motivated spectral indices $\alpha = 0$ and $\alpha = 2/3$, we identified prominent features in the CSD between the LHO and LLO strain data. These include mechanical resonances of optical components as well as intermodulation products of low-frequency calibration lines. These structures are also captured by the strict data-quality procedure described above.

c. High-frequency region ($400 - 900$ Hz*).* Several instrumental features in this band were found to drive excess power in steep spectral indices such as $\alpha = 5$. The main features in this band were associated with suspension violin modes and a time-dependent excess in the Livingston detector:

- Excess narrowband structure was observed around the fundamental suspension violin modes near 500 Hz. These modes are mechanical resonances of the quadruple suspension fibers, with higher-order harmonics appearing around 1000 Hz and above [108]. Throughout O4, during periods when the violin modes were excited, additional narrow spectral features appeared in nearby frequency bands. Narrowband spectral artifact studies found that many of these features were consistent with intermodulation involving violin modes, low-frequency calibration lines, and their harmonics [107].

- A broadband, time-dependent excess in LIGO Livingston between 540–640 Hz. Although auxiliary-channel studies showed modest correlations with the temperature monitoring channel at the corner stations, the exact source and coupling mechanism remain unidentified [104].

The strict notching procedure independently identifies these regions as exhibiting high temporal variability.

This methodology produces two distinct final notch lists: one for the O4a data set, differing from that reported in Ref. [75], and one for the O4b–O4c1 data set. Accordingly, we also report updated O1–O4a results in this paper that account for the stricter notch list. In total, we remove 22.2% of the 20–1726 Hz analysis band for O4a and 22.8% for O4b–O4c1, of which the strict notching procedure contributes an additional 2.1% and 4.5%, respectively.

D. Magnetic noise budget

As mentioned above, since searches for a GWB rely on correlations of strain data between spatially separated detectors, the analysis is susceptible to bias from correlated noise sources [89]. A well-known example is magnetic noise associated with Schumann resonances–global standing electromagnetic waves in the cavity formed by Earth's surface and the ionosphere, excited primarily by lightning activity [93, 109, 110]. Owing to their global nature, these resonances can induce correlated signals even between widely separated detectors [88].

Environmental magnetic fields can couple to the detector response through several mechanisms [111], including pickup in cables and other conductive components in the detector building, direct forces on the actuation magnets of the test-mass mirrors (as in Virgo [112]), and forces on magnets or magnetically susceptible material higher up in the test-mass suspension system (as in LIGO [88]). The strength of this coupling is quantified through coupling functions, namely the outside-to-inside and inside-to-strain transfer functions, capturing the couplings of magnetic field from outside the experimental buildings to inside the buildings and from inside the buildings to the strain detector channel, respectively. A detailed description of these quantities can be found in Sec. III F of Ref. [75]. For the outside-to-inside coupling functions, we adopt the same values and uncertainties used in the O4a and O3 magnetic noise budget analyses [75, 103]. For the inside-to-strain coupling, new values have been measured for each interferometer using the procedure described in Refs. [90, 112, 113].

The magnetometer calibration factors were remeasured during O4b, yielding values with improved accuracy (approximately 5% uncertainty) relative to those used in the O4a and O3 analyses, which had been derived prior to O3. The updated O4b measurements give calibration factors smaller than those from O3, corresponding to O3-to-O4 ratios of 1.26 for LHO in the magnetometer along the X arm and 1.24 along the Y arm. For LLO, the corresponding ratios are 4.07 and 3.24. This reduction results in a lower overall magnetic noise budget compared to the estimate for O4a.

The computation of the magnetic noise budget is described in detail in Sec. III F of Ref. [75], and the same approach is adopted in this work. Uncertainty estimation follows an identical procedure: the outside-to-inside coupling uncertainty measured during O3 at LLO is used, since equivalent measurements were not available for LHO or during O4. This is combined with a conservative intrinsic uncertainty factor of 2 to account for the mismatch between the location of the magnetometers in the building (used for the measurements) and the location where the magnetic field couples to the strain. The final magnetic noise budget is shown in Fig. 1. The calculated budget (blue solid curve) is compared with the 2σ power-law integrated (PI) sensitivity curve [114], obtained over the full O1–O4c1 observing period (black solid curve), which quantifies the sensitivity of the search to power law (PL) GWB. We also show the 2σ uncertainty on the O4b–O4c1 magnetic noise budget (red band). For comparison, the O4a magnetic noise budget is shown as a green solid line.

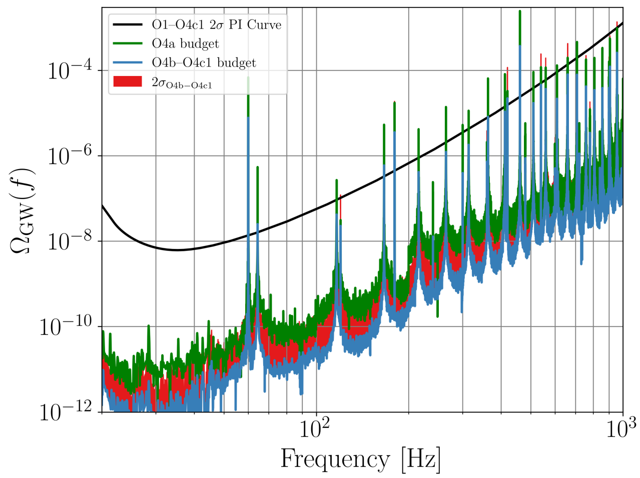

FIG. 1. Comparison of the magnetic noise budget calculated for O4a (green curve) and O4b–O4c1 (blue curve), which shows a difference in magnitude due to the remeasuring of the magnetometer calibration factors. The red band represents the 2σ uncertainty (shown only upwards) of the O4b–O4c1 budget.

E. Calibration uncertainties

Strain calibration uncertainties arise from both statistical fluctuations and systematic errors in the LVK detector strain calibration [115, 116].

In our Bayesian upper limits estimation, these uncertainties are incorporated by introducing a positive-definite calibration factor Λ in the likelihood, as described in Sec. III G of Ref. [75] (see also Refs. [87, 117] for additional details). The parameter Λ is marginalized over using the prior specified in Sec. III G of Ref. [75], with the corresponding calibration variance, σ_Λ, determined as described in Ref. [83]. Note that the calibration uncertainty modifies the variance of our estimator, as described in Eq. (5) of Ref. [118]. We then use this modified

Interferometer	O4b LHO	O4b LLO	O4c1 LHO	O4c1 LLO
Magnitude	4.7%	4.0%	13.3%	1.9%
Phase	2.6°	2.9°	6.4°	1.2°

TABLE II. Maximum strain calibration uncertainties at 68% credible level (CL) for the magnitude and phase of detector strain for O4b and O4c1.

variance for our estimator in the frequentist approach.

Table II summarizes the maximum uncertainties for the LHO and LLO detectors during O4b and O4c1. We note that the magnitude uncertainty at LHO during O4c1 is larger than usual. This is because, in the first part of O4c, high-frequency measurements at H1 were not available for certain time periods, resulting in reduced coverage above 1 kHz and correspondingly larger uncertainties in that frequency band. These uncertainties were later reduced in the second part of the third period of O4 (O4c2) once additional high-frequency measurements were included. While the overall quality of the O4c1 data is comparable to that of O4b, this effect is partly related to the way the data are analyzed in discrete detector epochs, within which the available calibration measurements vary depending on data availability at each stage. Importantly, we have verified that this increased uncertainty does not substantially affect our final Bayesian results.

As for the phase uncertainties, which remain below or close to $\lesssim 5°$, they do not introduce a significant bias in GWB analyses [119]. Therefore, our focus is on the magnitude component. By combining the magnitude uncertainties from each detector in quadrature, we obtain an overall calibration variance of $\sigma_\Lambda = 6.2\%$ during O4b and $\sigma_\Lambda = 13.4\%$ during O4c1.

III. RESULTS

We present the results obtained using the methodology described in Ref. [75], applied to data from the O4b and O4c1 observing periods in combination with data from the O1–O4a runs. No evidence for a GWB signal is found. Consequently, we set Bayesian upper limits on a range of models.

A. Frequentist results

We report in Table III the values of the broadband estimators $\hat{\Omega}_{\rm ref}$ [75] and their standard deviations for the O4b–O4c1 data set and the O1–O4c1 data set, evaluated at the 25 Hz reference frequency. We adopt three values of the spectral index (see Eq. (1)): $\alpha = 0$, corresponding to a scale-invariant signal such as a cosmological GWB from slow-roll inflation or cosmic strings [120]; $\alpha = 2/3$, consistent with an astrophysical GWB from compact binary coalescences (CBCs) [97]; and $\alpha = 3$, corresponding to a flat strain power spectrum [78].

For each spectral index, we also report the frequency $f_{99\%}$, defining the frequency range $[20, f_{99\%}]$ Hz within the $[20, 1726]$ Hz band that contributes to 99% of the search sensitivity.

The point estimates $\hat{\Omega}_{\rm ref}$ are consistent with zero within 1σ uncertainties for both the O4b–O4c1 data set and the combined O1–O4c1 data set, with the results for $\alpha = 0$ and $\alpha = 2/3$ exhibiting a marginally positive signal-to-noise ratio (SNR). We also show the cross-correlation spectrum from O1–O4c1 in $\Omega_{\rm GW}$ units in Fig. 2, together with the 1σ confidence regions from O4b–O4c1 and O1–O4c1. The cross-correlation spectrum and the 1σ confidence regions are consistent with zero, as expected for data dominated by uncorrelated Gaussian noise.

We also report updated results for the O1–O4a data set in Table III and Fig. 2, as we adopt a new (stricter) O4a notch list, as described in Sec. II. We find that the updated notch list has a mild impact on the uncertainties of the estimators. The corresponding values of $f_{99\%}^{\rm O1-O4a}$ also differ from those reported in Ref. [75].

B. Bayesian results

The data show no evidence for a signal; therefore, we set Bayesian upper limits at the 95% credible level (CL) based on the frequentist estimator result. These constraints are summarized in Table IV, and the corresponding posterior distributions are shown in Fig. 3. The solid lines show the posteriors obtained using a log-uniform prior on $\Omega_{\rm ref}$ and either a Gaussian (blue) or uniform (red) prior on α. The priors and models are the same as those used in Ref. [75].

For a log-uniform prior on $\Omega_{\rm ref}$ (see Eq. (1)), the log-Bayes factors comparing the signal and noise-only hypotheses are $\log_{10}\mathcal{B} = -0.518 \pm 0.009$ and $\log_{10}\mathcal{B} = -0.573 \pm 0.010$ for Gaussian and uniform priors on the spectral index α, respectively. These values indicate a preference for the noise-only hypothesis. The one-dimensional posterior for $\Omega_{\rm ref}$ shows no significant dependence on the choice of prior for α. Finally, the posterior for α no longer exhibits the peak around $\alpha = 5$ reported in Ref. [75]. This change arises from the investigations described in Sec. II, which identified additional noise features—now included in the notch list—that were responsible for the previously observed peak.

As noted above, the upper limits from O1–O4a reported in Table IV differ from those in Ref. [75] due to the adoption of a new notch list. While the updated frequency-domain cuts described in Sec. II do not substantially affect the O1–O4a sensitivity for spectral indices $\alpha = 0$, 2/3, 3, they do modify the broadband estimator values from the inverse-variance-weighting over the new set of frequencies. This leads to more conservative upper limits compared to those in Ref. [75] for the

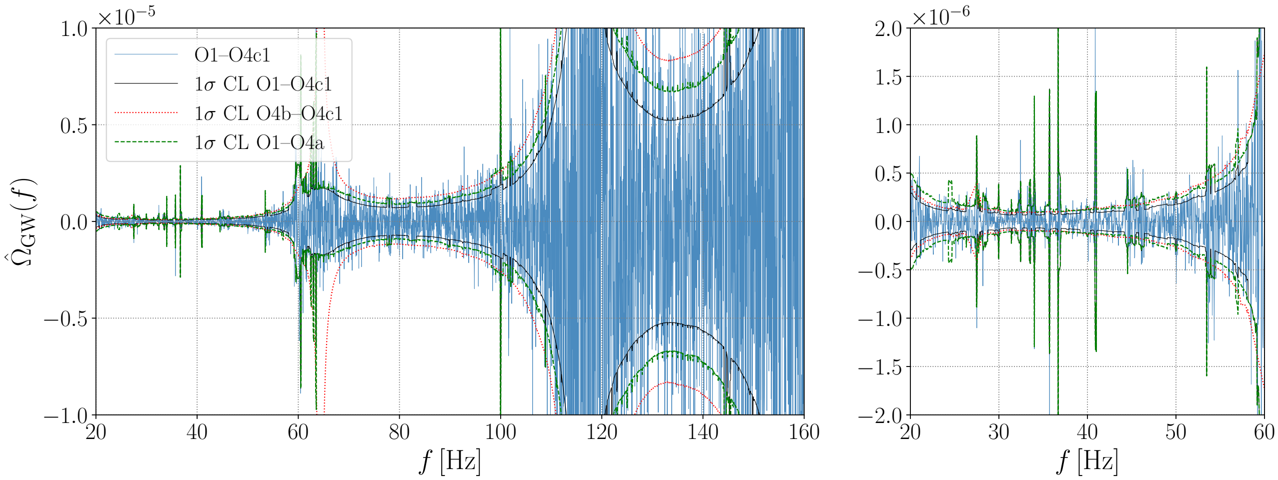

FIG. 2. Cross-correlation spectrum obtained from the combined O1–O4c1 data. The black solid lines denote the boundaries of the O1–O4c1 1σ region. The red dotted lines indicate the corresponding 1σ region for the O4b–O4c1 data alone, while the green dashed lines show the updated 1σ region for the O1–O4a data, reflecting the use of the stricter notch list relative to Ref. [75], as described in Sec. II. The spectrum (blue curve) remains consistent with zero across all frequency bins, showing no evidence for a GWB signal. The left panel shows the spectrum over the 20–160 Hz range, while the right panel focuses on frequencies below 60 Hz to emphasize the contribution from the O4b–O4c1 data in this band.

α	$f_{99\%}^{\rm O1-O4a}$ [Hz]	$\hat{\Omega}^{\rm O1-O4a}/10^{-9}$	$f_{99\%}^{\rm O4b-O4c1}$ [Hz]	$\hat{\Omega}^{\rm O4b-O4c1}/10^{-9}$	$f_{99\%}^{\rm O1-O4c1}$ [Hz]	$\hat{\Omega}^{\rm O1-O4c1}/10^{-9}$
0	64.7	1.1±4.8	53.3	0.3±4.9	56.2	0.7±3.4
2/3	87.6	0.4±3.6	84.2	−0.1±3.9	86.3	0.2±2.6
3	329.9	−0.3±0.6	347.9	−0.3±0.7	338.2	−0.3±0.5

TABLE III. Results from the isotropic search obtained with the standard cross-correlation optimal filter analysis, assuming PL spectra with indices $\alpha = \{0, 2/3, 3\}$. For each spectral index, we report the point estimate of the amplitude $\hat{\Omega}_{\rm ref}$ at 25 Hz together with its associated 1σ uncertainty. We also provide the frequency interval spanning from 20 Hz up to $f_{99\%}$, which contains 99% of the total sensitivity. The estimates are constructed by combining statistically independent frequency-bin measurements according to Eqs. (10) and (11) of Ref. [75]. The final two columns present the results obtained from the post-processing recombination of all observing runs (O1–O4c1), following the methodology of Ref. [103]. We note that Virgo data contribute to the O3 measurements, leading to three independent baseline contributions in that observing period. We have also included the results from the combination of data from O1 to O4a, an update of the results presented in Ref. [75].

spectral indices $\alpha = 0$ and $2/3$.

We find that the upper limits from O1–O4c1 are more stringent than those from O1–O4a by a factor of 1.3 to 1.5 for both uniform and log-uniform priors on $\Omega_{\rm ref}$.

C. Non-GR polarizations

Following the Bayesian framework adopted in Ref. [75], and based on the formalism introduced in Ref. [96], we perform a search aimed at improving constraints on possible deviations from GR [95]. The detection of non-tensorial polarization modes would provide direct evidence for a violation of GR, while their non-observation enables us to place limits on extended theories of gravity.

We adopt different models corresponding to GWBs with different polarization content. In particular, we first consider a mixed-polarization background, as described in Sec. II C of Ref. [75], allowing for tensor, vector, and scalar components. We adopt log-uniform priors on the amplitude parameters $\Omega_{\rm ref,(p)}$, with $({\rm p}) \in \{{\rm T}, {\rm V}, {\rm S}\}$, over the range 10^{-13}–10^{-6}, and Gaussian priors on the spectral indices $\alpha_{\rm ref,(p)}$, with $({\rm p}) \in \{{\rm T}, {\rm V}, {\rm S}\}$, centered at zero with a standard deviation of 3.5. From this analysis, we derive 95% credible level upper limits on $\Omega_{\rm ref,(p)}$, summarized in the second column of Table V.

As described previously, the upper limits reported in Ref. [75] are not directly comparable to the updated results presented here. We therefore recompute the O1–O4a upper limits using the stricter notch list described in Sec. II, obtaining the values reported in column 3 of Table V. This yields improvements in the O1–O4c1 upper limits, with respect to the recomputed O1–O4a results, by factors of 1.5, 1.4, and 1.3 for the tensor, vector, and scalar polarizations, respectively.

The upper limit for the scalar-polarized case remains less stringent because the scalar overlap reduction function is approximately three times smaller in amplitude than the corresponding tensor and vector functions [96]. Consequently, the detector network is less sensitive to a

	Uniform prior			Log-uniform prior		
α	**O1–O4c1**	**O1–O4a**	**Improvement**	**O1–O4c1**	**O1–O4a**	**Improvement**
0	7.4×10^{-9}	1.1×10^{-8}	1.5	2.8×10^{-9}	3.9×10^{-9}	1.4
2/3	5.5×10^{-9}	7.9×10^{-9}	1.4	2.0×10^{-9}	2.8×10^{-9}	1.4
3	7.5×10^{-10}	1.0×10^{-9}	1.3	2.6×10^{-10}	3.6×10^{-10}	1.4
Marginalized	1.1×10^{-8}	1.7×10^{-8}	1.5	2.7×10^{-9}	4.1×10^{-9}	1.5

TABLE IV. Bayesian upper limits at 95% CL on the GWB amplitude $\Omega_{\rm ref}$ assuming uniform (left) and log-uniform (right) priors. Results obtained using O1–O4c1 data are compared with previous constraints from O1–O4a data. Limits are reported for fixed values of the spectral index α and for the case in which α is marginalized over assuming a Gaussian prior. The improvement relative to O1–O4a ranges from factors of 1.3 to 1.5 over the different priors and spectral indices. The O1–O4a upper limits differ from those in Ref. [75], due to the updated notch list, as described in Sec. II.

Polarization	**O1–O4c1**	**O1–O4a (updated)**	**Improvement**
Tensor	2.7×10^{-9}	3.9×10^{-9}	1.5
Vector	2.7×10^{-9}	3.7×10^{-9}	1.4
Scalar	6.9×10^{-9}	9.3×10^{-9}	1.3

TABLE V. 95% CL upper limits on the amplitude of each polarization (p) component ($\Omega_{\rm ref,p}(25\,{\rm Hz})$) for a mixed-polarization background. Relative to the updated O1–O4a results, which supersede those reported in Ref. [75], the limits improve by factors of 1.3–1.5. The upper limit on the scalar component remains less stringent because of its smaller overlap reduction function [96].

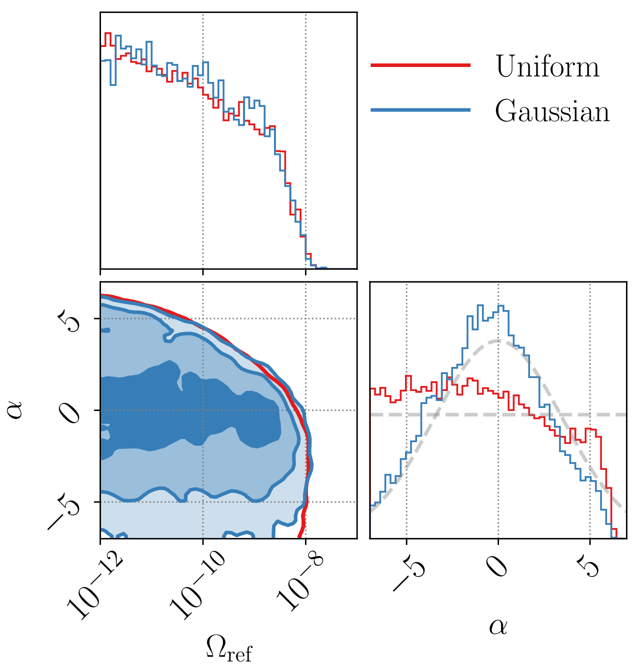

FIG. 3. Posterior distributions on the PL model parameters $\{\Omega_{\rm ref}, \alpha\}$ describing a GWB under the assumptions of a log-uniform prior on $\Omega_{\rm ref}$ and either a Gaussian (blue curve) or a uniform (red curve) prior on α, with the α priors in the corresponding one-dimensional histogram (gray dashed lines). The blue shaded regions indicate the 1, 2, and 3σ credible intervals, from darkest to lightest.

scalar-polarized GWB.

We also perform dedicated searches under the assumption of purely tensor, vector, and scalar backgrounds, obtaining 95% credible upper limits of $\Omega_{\rm ref,T}(25\,{\rm Hz}) \leq 2.6\times 10^{-9}$, $\Omega_{\rm ref,V}(25\,{\rm Hz}) \leq 3.0 \times 10^{-9}$, and $\Omega_{\rm ref,S}(25\,{\rm Hz}) \leq 7.5 \times 10^{-9}$, respectively, when marginalizing over the spectral index. Relative to the updated O4a results, these correspond to improvements by factors of 1.5, 1.3, and 1.2 for the tensor, vector, and scalar polarizations.

As explained in Ref. [75], the upper limits remain comparable across polarization because the O4 analysis uses only the LHO–LLO baseline, unlike O3 where the inclusion of Virgo data improved the ability to distinguish among different polarization modes.

To quantify the evidence for a stochastic signal, we compute the Bayes factor comparing the signal and noise hypotheses as $\frac{1}{7}\sum_{\mathcal{H}} \mathcal{B}^{\mathcal{H}}_{\rm N}$ for $\mathcal{H} \in \{{\rm T, V, S, TV, TS, VS, TVS}\}$ obtaining $\log_{10}\mathcal{B} = -0.947 \pm 0.004$ at 68% credibility (see Appendix C of Ref. [96]), which indicates no statistically significant evidence for a detection. Here, the signal hypothesis is defined as an equal-weighted mixture of the tensor, vector, and scalar components, as well as their pairwise and triply combined configurations (TV, TS, VS, and TVS), thereby treating all polarization scenarios on an equal footing. Finally, we evaluate the Bayes factor comparing non-GR and GR-consistent polarization models yielding $\log_{10}\mathcal{B} = -0.498 \pm 0.010$ at 68% credibility. This result indicates a preference for a tensor-polarized background, as predicted by GR, over vector, scalar, and mixed-polarization alternatives. However, in the absence of a detection, this preference is expected to be dominated by the Occam penalty associated with the additional unconstrained parameters introduced in the more complex models.

D. Joint magnetic and stochastic analysis

To ensure that the effect of the contamination from correlated magnetic noise is negligible on the search for a GWB, we provide a complementary test by performing a Bayesian analysis with the O4b and O4c1 data on a joint model composed of correlated magnetic noise and a GWB signal described by a power law (PL). Following the methodology of Ref. [121], we compute the CSD of the magnetic channels between the two detectors. The inside-to-strain transfer functions (see Ref. [75] for a detailed description of this transfer function) are modelled using a PL approximation. These components are then combined to estimate the equivalent fractional energy density associated with correlated magnetic noise.

Since we only include LHO and LLO data, the amplitudes $\kappa_{H,L}$ and spectral indices $\beta_{H,L}$ of the coupling functions described in Eq. (20) of Ref. [75] are degenerate. Therefore, to avoid the degeneracy in the Bayesian analysis, we adopt the amplitude product $\kappa_{HL} = \kappa_H \kappa_L$ and index sum $\beta_{HL} = \beta_H + \beta_L$ as the non-degenerate parameters of the correlated magnetic noise model.

In contrast to the magnetic budget, which relies on measured transfer functions from the magnetic field to the strain channel, this additional analysis aims to estimate the impact of correlated magnetic noise using agnostic priors for κ_{HL} and β_{HL} that are independent of transfer function measurements. Instead of setting priors driven by such measured transfer functions as in the O3 and O4a analyses [75, 103], we have substantially expanded the range of the prior distributions for κ_{HL} and β_{HL} compared with those adopted in the previous analysis to cover the detection sensitivity shown by the O1–O4a PI curve, thereby making this estimation more conservative. Consequently, we adopt a log-uniform prior distribution, ranging from 10^{-56} to $10^{-38}\,\mathrm{pT}^{-2}$, for κ_{HL} and a uniform prior from -4 to 22 for β_{HL} [103].

We estimate the evidence for a magnetic noise only model and a joint model of magnetic noise and a PL GWB signal. The Bayes factor comparing the magnetic noise only model to the uncorrelated Gaussian noise model is $\log_{10}\mathcal{B}_N^{\mathrm{MAG}} = -0.185 \pm 0.003$, which indicates the absence of correlated magnetic noise in the narrow band point estimate spectra. The Bayes factor comparing the joint model of magnetic noise and a PL GWB signal to the uncorrelated Gaussian noise model is $\log_{10}\mathcal{B}_N^{\mathrm{PL+MAG}} = -0.400 \pm 0.004$, verifying the null result for detecting both the PL GWB signal and correlated magnetic noise.

IV. ASTROPHYSICAL IMPLICATIONS

To interpret our upper limits, we place them in the context of the astrophysical GWB expected from the population of compact binary mergers inferred from the most recent LVK catalog, GWTC-5.0 [122]. Note that this analysis includes GW events detected up to the end of O4b, as a GWTC-6.0 catalog incorporating O4c events is not yet available. In the frequency band of interest, the CBC background is expected to dominate the isotropic GWB. Following the O4a update [75], we compute the contributions from BBH, BNS and NSBH systems at the 90% credible level based on recent GW observations. For the BBH population, we perform hierarchical Bayesian population inference and propagate the inferred hyperposterior into predictions for $\Omega_{\mathrm{GW}}(f)$. We adopt the same strongly parameterized population model used in Refs. [99, 123]. In this model, the primary mass distribution is described by a broken PL between 3 and 200 $M_\odot$ with two Gaussian peaks at $\sim 10\,M_\odot$ and $\sim 35\,M_\odot$, and tapering applied at the low-mass end to ensure a smooth turn-on of the distribution. The mass ratio follows a PL, spin magnitudes are drawn from a truncated normal distribution, and spin tilts are modeled as a mixture of isotropic and preferentially aligned configurations. As in Ref. [75], but in contrast to the PL redshift evolution assumed in Ref. [99], we employ a generic broken PL redshift model that allows for a turnover in the merger rate history,

$$R_{\mathrm{BBH}}(z) = C(\alpha_z, \beta_z, z_{\mathrm{p}}) \frac{R_0 (1+z)^{\alpha_z}}{1 + \left(\frac{1+z}{1+z_{\mathrm{p}}}\right)^{\alpha_z + \beta_z}}, \tag{3}$$

where α_z and β_z characterize the low- and high-redshift slopes, respectively, and z_{p} denotes the turnover redshift at which the merger rate density transitions from its low-redshift rise to its high-redshift decline. The normalization constant $C(\alpha_z, \beta_z, z_{\mathrm{p}})$ ensures that the merger rate density is normalized to the local rate $R_{\mathrm{BBH}}(0) = R_0$. This redshift model is motivated by the fact that high-redshift sources can contribute substantially to the GWB and theoretical models of the merger rate evolution generally predict a turnover [2, 124, 125]. Using the same priors on the mass and spin distributions as in Ref. [99], together with the redshift-evolution priors as in the O4a analysis [75], we recover mass and spin distributions that are fully consistent with the GWTC-5.0 population study [99]. We infer a local BBH merger rate of $R_0 = 18.4^{+5.1}_{-4.2}\,\mathrm{Gpc}^{-3}\mathrm{yr}^{-1}$, which is likewise consistent with the results reported in Ref. [99], noting that the BBH merger rates quoted therein are evaluated at $z = 0.2$. While the high-redshift slope β_z remains unconstrained, we obtain positive values for the low-redshift index $\alpha_z = 2.7^{+0.9}_{-0.7}$, which are somewhat lower than those reported in the O4a analysis. We also find a mild preference for turnover redshifts $z_{\mathrm{p}} \simeq 2$, with very low values of z_{p} disfavored. This shift towards a more moderate increase of the BBH merger rate with redshift, also consistently observed in Ref. [99], results in a credible band that is overall shifted to lower merger rates compared to O4a, as illustrated in Fig. 4.

Following the procedure outlined in Refs. [75, 126, 127], we compute the fractional energy density spectrum for each posterior sample of the BBH population model. In

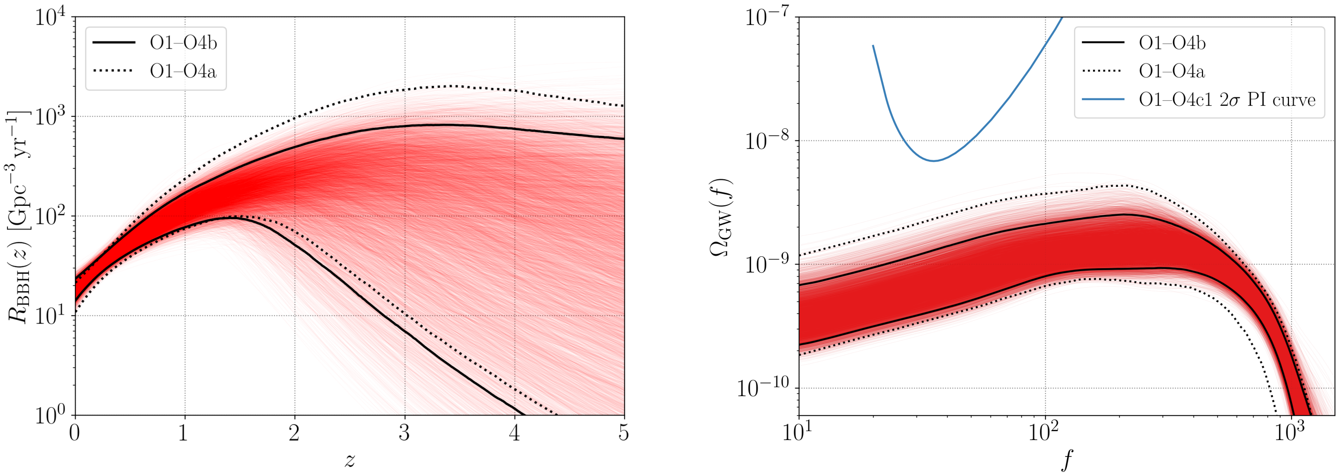

FIG. 4. *Left panel:* Redshift evolution of the BBH merger rate density, inferred hierarchically from the BBH detections in GWTC-5.0, spanning observing runs O1–O4b. The red traces show the individual posterior samples, while the solid black lines indicate the 90% credible bounds. For comparison, the 90% credible bounds obtained previously with GWTC-4.0, which includes events through O4a, are shown as dotted lines. *Right panel:* Prediction of the stochastic energy-density spectrum of the BBH population. The red traces correspond to the individual posterior samples on the energy-density spectrum obtained by sampling over the possible mass, spin and redshift distributions of BBH mergers, while the solid black curves indicate 90% credible bounds on $\Omega_{\rm BBH}(f)$. For comparison, we also indicate the 90% credible bounds obtained after O4a with dotted lines as presented in Ref. [75]. Furthermore, we show the 2σ PI sensitivity curve from O1–O4c1 data.

the absence of a stochastic detection, we apply the rejection sampling method of Ref. [75] to combine constraints from direct BBH detections with those from the stochastic search [128]. The individual $\Omega_{\rm BBH}(f)$ spectra are retained or rejected based on their consistency with the measured cross-correlation data. Because the majority of the spectra lie well below the search upper limits, only a small fraction of samples is rejected. The resulting ensemble of accepted spectra, together with the corresponding 90% credible band, is shown in Fig. 4. At the reference frequency of 25 Hz, we obtain a predicted BBH background amplitude of $\Omega_{\rm BBH}(25\,{\rm Hz}) = 5.6^{+5.0}_{-2.1}\times10^{-10}$. This represents a substantial improvement over previous constraints: although the lower bound remains similar, the upper bound is reduced by almost a factor of two. This tightening primarily arises from the improved constraints on the BBH merger-rate density, in particular on the low-redshift slope α_z. Looking ahead, we expect the growing catalog of directly detected BBH mergers to further tighten constraints on R_0, α_z and the low-redshift side of $z_{\rm p}$. In contrast, stochastic background measurements will provide complementary information on the merger rate density at higher redshifts, constraining β_z and the high-redshift side of $z_{\rm p}$.

Beyond the BBH contribution, we also predict the GWB generated by BNS and NSBH systems, following the same procedure as in Ref. [75]. Owing to the limited constraints from direct observations of these populations, we estimate their local rates under fixed assumptions about their mass and spin distributions, and we model their redshift evolution by convolving the cosmic star-formation history with a distribution of delay times between formation and merger. Specifically, we assume that progenitor formation traces the star-formation rate density of Ref. [129] and that delay times are distributed log-uniformly between 20 Myr and 13.5 Gyr. For the BNS population, we adopt a uniform component mass distribution between 1 and 2.5 $M_\odot$ and isotropic spin orientations with spin magnitudes uniformly distributed below 0.4. Under these assumptions, we infer a local BNS merger rate of $38^{+69}_{-30}\,{\rm Gpc}^{-3}{\rm yr}^{-1}$. This estimate is consistent with the BNS merger rate reported in Ref. [99], although that analysis jointly inferred the BNS and BBH merger rates across the full compact binary mass range. Using this merger rate, we predict a BNS background amplitude of $\Omega_{\rm BNS}(25\,{\rm Hz}) = 2.3^{+4.1}_{-1.8}\times10^{-11}$, with the dominant uncertainty arising from the local merger rate.

For NSBH systems, we assume that the neutron-star component follows the same mass and spin distributions as in the BNS population, while the black-hole component is drawn from a log-uniform mass distribution between 3 and 50 $M_\odot$, with isotropically oriented spins and magnitudes uniformly distributed below 0.99. These assumptions yield a local NSBH merger rate of $22^{+24}_{-14}\,{\rm Gpc}^{-3}{\rm yr}^{-1}$, and a corresponding stochastic background amplitude of $\Omega_{\rm NSBH}(25\,{\rm Hz}) = 3.6^{+4.0}_{-2.3}\times10^{-11}$. Figure 5 shows the resulting 90% credible intervals for the BNS and NSBH backgrounds alongside the BBH contribution. For both BNS and NSBH, the credible bands narrow relative to earlier estimates, primarily due to the improved constraints on their local merger rates.

We also combine the individual BBH, BNS and NSBH forecasts to obtain a total CBC background estimate, for which we find $\Omega_{\rm CBC}(25\,{\rm Hz}) = 6.3^{+5.0}_{-2.2}\times10^{-10}$. The

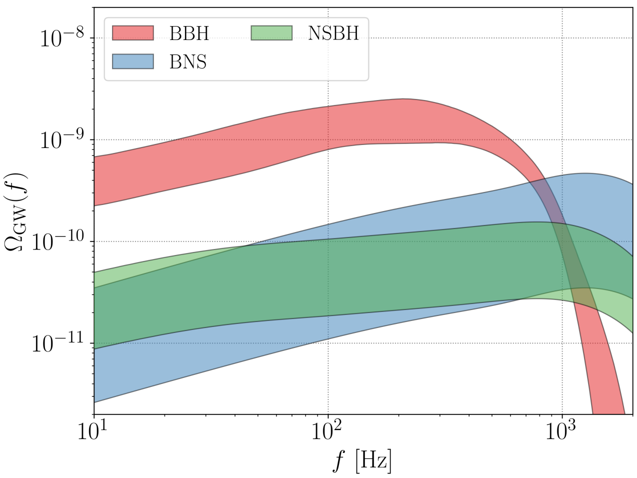

FIG. 5. Predicted astrophysical GWBs from BBH, BNS and NSBH coalescences at the 90% credible level.

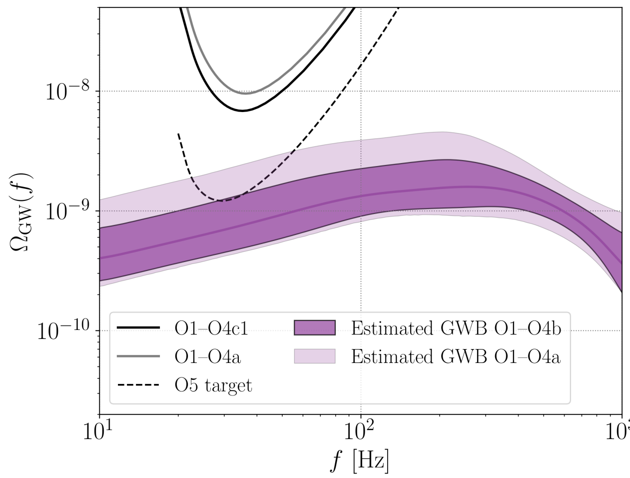

FIG. 6. The purple band shows the combined estimate of the CBC background at the 90% credible level, with the median indicated by the solid line. For comparison, the previous estimate after O4a from Ref. [75] is also shown. The figure further includes the 2σ PI sensitivity curve of the O1–O4c1 search presented in this work, together with the corresponding curve from the O4a search and the projected target sensitivity for one year of coincident O5 data. The O5 projection assumes equal observing time at the expected O5a, O5b and O5c sensitivity levels.

upper bound of this credible interval is roughly a factor of two lower than the value reported in the previous LVK stochastic background search [75], mainly due to the weaker rise of the BBH merger rate evolution at low redshift, as discussed above. Figure 6 shows the combined estimate alongside the 2σ PI curve representing the integrated sensitivity of the search reported here, as well as the updated projected O5 sensitivity of the LIGO detectors [100]. Since the O5 sensitivity projection is provided for three representative epochs with progressively improving sensitivity levels, the O5 PI curve shown here is constructed assuming one year of coincident data, with one third of the observing time spent at each of the O5a, O5b and O5c sensitivity levels. With the increased number of GW observations and the improved understanding of the local CBC populations, the uncertainty on our CBC background estimate is substantially reduced. Nevertheless, under the projected O5 sensitivity, a detection of the CBC background remains within reach, provided the detectors achieve their anticipated performance.

V. CONCLUSIONS

In this work, we performed a cross-correlation search for an isotropic gravitational-wave background using data from the first LVK observing run (O1) through April 1, 2025 (O4c1). Relative to the previous analysis in Ref. [75], this search incorporated an additional 117 days of coincident LIGO Hanford–Livingston data from O4b and O4c1, after data-quality cuts. We did not include Virgo data from O4, as their addition improved the network sensitivity by less than 1%. The analysis covered the frequency band from 20 to 1726 Hz.

During O4, new data-quality challenges emerged in the form of noise features not identified by existing vetoing methods. To address this, we developed a stricter notch-list procedure based on the temporal variability of the power spectral density, which allowed us to identify both narrow spectral lines and broader non-stationary features that remained hidden in time-averaged spectra. This produced two new notch lists: an updated one for O4a and another for O4b–O4c1, which made it necessary to reanalyze the O1–O4a data with the revised frequency cuts.

We found no evidence for an isotropic background. Hence, we placed a 95% credible upper limit of e.g. $\Omega_{\rm ref}(25\,{\rm Hz}) \leq 2.8 \times 10^{-9}$ for a spectral index $\alpha = 0$ under a log-uniform prior ($\leq 7.4 \times 10^{-9}$ under a uniform prior), improving the recalculated O1–O4a constraints by a factor of 1.4 (1.5 for a uniform prior).

Since cross-correlation searches could be biased by correlated environmental noise, we also evaluated the contribution from magnetic Schumann resonances and found that correlated magnetic noise did not affect the results in this paper. Furthermore, we performed a joint Bayesian search in which correlated magnetic noise and the gravitational-wave background were assumed to be present simultaneously, which showed no evidence for such a scenario.

We also searched for alternative gravitational-wave polarizations beyond the tensor modes predicted by general relativity, namely scalar and vector components. We improved O1–O4a constraints on these non-standard polarization backgrounds by factors of 1.4 and 1.3 for vector and scalar modes, respectively. Our analysis indicated a preference for a tensor-polarized background, as predicted by GR. However, in the absence of a detection, this apparent preference is expected to be driven primarily by the Occam penalty associated with the additional unconstrained parameters of the more complex polarization models.

We updated the forecast of the GWB from compact binaries using population inferences based on GWTC-5.0. By propagating uncertainties in the population models, we obtained refined estimates for the BBH, BNS and NSBH contributions and combined them into an updated prediction for the total CBC background. The inferred background amplitude is lower and more tightly constrained than in previous analyses, primarily due to improved measurements of the BBH merger-rate evolution, including evidence for a more moderate increase with redshift. While current observational limits remain above the predicted astrophysical background, the expected sensitivity improvements in O5 make a detection of the CBC background increasingly plausible, positioning stochastic searches as a complementary probe of compact binary formation and merger history across cosmic time.

ACKNOWLEDGMENTS

This material is based upon work supported by NSF's LIGO Laboratory, which is a major facility fully funded by the National Science Foundation. This publication has been assigned LIGO document number P2600217. The authors also gratefully acknowledge the support of the Science and Technology Facilities Council (STFC) of the United Kingdom, the Max-Planck-Society (MPS), and the State of Niedersachsen/Germany for support of the construction of Advanced LIGO and construction and operation of the GEO 600 detector. Additional support for Advanced LIGO was provided by the Australian Research Council. The authors gratefully acknowledge the Italian Istituto Nazionale di Fisica Nucleare (INFN), the French Centre National de la Recherche Scientifique (CNRS) and the Netherlands Organization for Scientific Research (NWO) for the construction and operation of the Virgo detector and the creation and support of the EGO consortium. The authors also gratefully acknowledge research support from these agencies as well as by the Council of Scientific and Industrial Research of India, the Department of Science and Technology, India, the Science & Engineering Research Board (SERB), India, the Ministry of Human Resource Development, India, the Spanish Agencia Estatal de Investigación (AEI), the Spanish Ministerio de Ciencia, Innovación y Universidades, the European Union NextGenerationEU/PRTR (PRTR-C17.I1), the ICSC - CentroNazionale di Ricerca in High Performance Computing, Big Data and Quantum Computing, funded by the European Union NextGenerationEU, the Comunitat Autonòma de les Illes Balears through the Conselleria d'Educació i Universitats, the Conselleria d'Innovació, Universitats, Ciència i Societat Digital de la Generalitat Valenciana and the CERCA Programme Generalitat de Catalunya, Spain, the Polish National Agency for Academic Exchange, the National Science Centre of Poland and the European Union - European Regional Development Fund; the Foundation for Polish Science (FNP), the Polish Ministry of Science and Higher Education, the Swiss National Science Foundation (SNSF), the Russian Science Foundation, the European Commission, the European Social Funds (ESF), the European Regional Development Funds (ERDF), the Royal Society, the Scottish Funding Council, the Scottish Universities Physics Alliance, the Hungarian Scientific Research Fund (OTKA), the French Lyon Institute of Origins (LIO), the Belgian Fonds de la Recherche Scientifique (FRS-FNRS), Actions de Recherche Concertées (ARC) and Fonds Wetenschappelijk Onderzoek - Vlaanderen (FWO), Belgium, the Paris Île-de-France Region, the National Research, Development and Innovation Office of Hungary (NKFIH), the National Research Foundation of Korea, the Natural Sciences and Engineering Research Council of Canada (NSERC), the Canadian Foundation for Innovation (CFI), the Brazilian Ministry of Science, Technology, and Innovations, the International Center for Theoretical Physics South American Institute for Fundamental Research (ICTP-SAIFR), the Research Grants Council of Hong Kong, the National Natural Science Foundation of China (NSFC), the Israel Science Foundation (ISF), the US-Israel Binational Science Fund (BSF), the Leverhulme Trust, the Research Corporation, the National Science and Technology Council (NSTC), Taiwan, the United States Department of Energy, and the Kavli Foundation. The authors gratefully acknowledge the support of the NSF, STFC, INFN and CNRS for provision of computational resources. This work was supported by MEXT, the JSPS Leading-edge Research Infrastructure Program, JSPS Grant-in-Aid for Specially Promoted Research 26000005, JSPS Grant-in-Aid for Scientific Research on Innovative Areas 2402: 24103006, 24103005, and 2905: JP17H06358, JP17H06361 and JP17H06364, JSPS Core-to-Core Program A. Advanced Research Networks, JSPS Grants-in-Aid for Scientific Research (S) 17H06133 and 20H05639, JSPS Grant-in-Aid for Transformative Research Areas (A) 20A203: JP20H05854, the joint research program of the Institute for Cosmic Ray Research, University of Tokyo, the National Research Foundation (NRF), the Computing Infrastructure Project of the Global Science experimental Data hub Center (GSDC) at KISTI, the Korea Astronomy and Space Science Institute (KASI), the Ministry of Science and ICT (MSIT) in Korea, Academia Sinica (AS), the AS Grid Center (ASGC) and the National Science and Technology Council (NSTC) in Taiwan under grants including the Science Vanguard Research Program, the Advanced Technology Center (ATC) of NAOJ, the Mechanical Engineering Center of KEK and Vietnam National Foundation for Science and Technology Development (NAFOSTED) 103.01-2025.147. Additional acknowledgements for support of individual authors may be found in the following document:

---

[1] S. Marassi, R. Schneider, G. Corvino, V. Ferrari, and S. P. Zwart, Phys. Rev. D **84**, 124037 (2011).
[2] X.-J. Zhu, E. Howell, T. Regimbau, D. Blair, and Z.-H. Zhu, Astrophys. J. **739**, 86 (2011).
[3] P. A. Rosado, Phys. Rev. D **84**, 084004 (2011).
[4] C. Wu, V. Mandic, and T. Regimbau, Phys. Rev. D **85**, 104024 (2012).
[5] X.-J. Zhu, E. Howell, D. Blair, and Z.-H. Zhu, Mon. Not. R. Astron. Soc. **431** (2012), 10.1093/mnras/stt207.
[6] A. Buonanno, G. Sigl, G. G. Raffelt, H.-T. Janka, and E. Müller, Phys. Rev. D **72**, 084001 (2005).
[7] P. Sandick, K. A. Olive, F. Daigne, and E. Vangioni, Phys. Rev. D **73**, 104024 (2006).
[8] K. Crocker, V. Mandic, T. Regimbau, K. Belczynski, W. Gladysz, K. Olive, T. Prestegard, and E. Vangioni, Phys. Rev. D **92** (2015), 10.1103/PhysRevD.92.063005.
[9] K. Crocker, T. Prestegard, V. Mandic, T. Regimbau, K. Olive, and E. Vangioni, Phys. Rev. D **95**, 063015 (2017).
[10] V. Ferrari, S. Matarrese, and R. Schneider, Mon. Not. R. Astron. Soc. **303**, 258 (1999).
[11] X.-J. Zhu, X.-L. Fan, and Z.-H. Zhu, Astrophys. J. **729**, 59 (2011).
[12] P. A. Rosado, Phys. Rev. D **86**, 104007 (2012).
[13] P. D. Lasky, M. F. Bennett, and A. Melatos, Phys. Rev. D **87**, 063004 (2013).
[14] A. Arvanitaki and S. Dubovsky, Phys. Rev. D **83**, 044026 (2011).
[15] R. Brito, V. Cardoso, and P. Pani, Lect. Notes Phys. **906**, pp.1 (2015).
[16] M. Sasaki, T. Suyama, T. Tanaka, and S. Yokoyama, Phys. Rev. Lett. **117**, 061101 (2016).
[17] R. Brito, S. Ghosh, E. Barausse, E. Berti, V. Cardoso, I. Dvorkin, A. Klein, and P. Pani, Phys. Rev. Lett. **119**, 131101 (2017).
[18] T. Takahashi, H. Omiya, and T. Tanaka, Phys. Rev. D **110**, 104038 (2024).
[19] T. W. B. Kibble, J. Phys. A: Math. Gen. **9**, 1387 (1976).
[20] T. Vachaspati and A. Vilenkin, Phys. Rev. D **31**, 3052 (1985).
[21] M. B. Hindmarsh and T. W. B. Kibble, Rep. Prog. Phys. **58**, 477 (1995).
[22] T. Damour and A. Vilenkin, Phys. Rev. Lett. **85**, 3761 (2000).
[23] T. Damour and A. Vilenkin, Phys. Rev. D **71**, 063510 (2005).
[24] X. Siemens, V. Mandic, and J. Creighton, Phys. Rev. Lett. **98**, 111101 (2007).
[25] S. Olmez, V. Mandic, and X. Siemens, Phys. Rev. D **81**, 104028 (2010).
[26] M. Kawasaki, K. Miyamoto, and K. Nakayama, Phys. Rev. D **81**, 103523 (2010).
[27] T. Vachaspati, L. Pogosian, and D. Steer, Scholarpedia **10**, 31682 (2015).
[28] J. J. Blanco-Pillado and K. D. Olum, Phys. Rev. D **96**, 104046 (2017).
[29] B. P. Abbott, R. Abbott, T. D. Abbott, F. Acernese, K. Ackley, C. Adams, T. Adams, P. Addesso, R. X. Adhikari, *et al.* (LIGO Scientific Collaboration and Virgo Collaboration), Phys. Rev. D **97**, 102002 (2018).
[30] P. Auclair *et al.*, JCAP **04**, 034 (2020).
[31] R. Abbott, T. D. Abbott, S. Abraham, F. Acernese, K. Ackley, A. Adams, C. Adams, R. X. Adhikari, V. B. Adya, and C. Affeldt (LIGO Scientific Collaboration, Virgo Collaboration, and KAGRA Collaboration), Phys. Rev. Lett. **126**, 241102 (2021).
[32] K. Schmitz and T. Schröder, Phys. Rev. D **110** (2024), 10.1103/PhysRevD.110.063549.
[33] E. Witten, Phys. Rev. D **30**, 272 (1984).
[34] C. J. Hogan, Mon. Not. Roy. Astron. Soc. **218**, 629 (1986).
[35] M. S. Turner and F. Wilczek, Phys. Rev. Lett. **65**, 3080 (1990).
[36] A. Kosowsky, M. S. Turner, and R. Watkins, Phys. Rev. D **45**, 4514 (1992).
[37] M. Kamionkowski, A. Kosowsky, and M. S. Turner, Phys. Rev. D **49**, 2837 (1994).
[38] A. Mazumdar and G. White, Rept. Prog. Phys. **82**, 076901 (2019).
[39] M. B. Hindmarsh, M. Lüben, J. Lumma, and M. Pauly, SciPost Phys. Lect. Notes **24**, 1 (2021).
[40] A. Romero, K. Martinovic, T. A. Callister, H.-K. Guo, M. Martínez, M. Sakellariadou, F.-W. Yang, and Y. Zhao, Phys. Rev. Lett. **126**, 151301 (2021).
[41] C. Badger, B. Fornal, K. Martinovic, A. Romero, K. Turbang, H.-K. Guo, A. Mariotti, M. Sakellariadou, A. Sevrin, F.-W. Yang, and Y. Zhao, Phys. Rev. D **107**, 023511 (2023).
[42] B. J. Carr, Astrophys. J. **201**, 1 (1975).
[43] M. Raidal, V. Vaskonen, and H. Veermäe, JCAP **09**, 037 (2017).
[44] B. Carr, K. Kohri, Y. Sendouda, and J. Yokoyama, Rept. Prog. Phys. **84**, 116902 (2021).
[45] T. Boybeyi, S. Clesse, S. Kuroyanagi, and M. Sakellariadou, Phys. Rev. D **112**, 023551 (2025).
[46] S. Matarrese, S. Mollerach, and M. Bruni, Phys. Rev. D **58**, 043504 (1998).
[47] D. Baumann, P. J. Steinhardt, K. Takahashi, and K. Ichiki, Phys. Rev. D **76**, 084019 (2007).
[48] K. Kohri and T. Terada, Phys. Rev. D **97**, 123532 (2018).
[49] A. Romero-Rodríguez, M. Martínez, O. Pujolàs, M. Sakellariadou, and V. Vaskonen, Phys. Rev. Lett. **128**, 051301 (2022).
[50] R. Inui, S. Jaraba, S. Kuroyanagi, and S. Yokoyama, J. Cosmol. Astropart. Phys. **2024** (2024), 10.1088/1475-7516/2024/05/082.
[51] S. Mukherjee and J. Silk, Mon. Not. Roy. Astron. Soc. **506**, 3977 (2021).

[52] M. Giovannini, Phys. Rev. D **58**, 083504 (1998).
[53] M. Giovannini, Phys. Rev. D **60**, 123511 (1999).
[54] D. G. Figueroa and E. H. Tanin, JCAP **10**, 050 (2019).
[55] D. G. Figueroa and E. H. Tanin, JCAP **08**, 011 (2019).
[56] H. Duval, S. Kuroyanagi, A. Mariotti, A. Romero-Rodríguez, and M. Sakellariadou, Phys. Rev. D **110**, 103503 (2024).
[57] A. A. Starobinsky, JETP Lett. **30**, 682 (1979).
[58] V. F. Mukhanov and G. V. Chibisov, JETP Lett. **33**, 532 (1981).
[59] L. Abbott and M. B. Wise, Nucl. Phys. B **244**, 541 (1984).
[60] N. Barnaby, E. Pajer, and M. Peloso, Phys. Rev. D **85**, 023525 (2012).
[61] N. Barnaby, R. Namba, and M. Peloso, JCAP **04**, 009 (2011).
[62] A. Maleknejad, JHEP **07**, 104 (2016).
[63] N. Bartolo *et al.*, JCAP **12**, 026 (2016).
[64] B. Thorne, T. Fujita, M. Hazumi, N. Katayama, E. Komatsu, and M. Shiraishi, Phys. Rev. D **97**, 043506 (2018).
[65] C. Badger, H. Duval, T. Fujita, S. Kuroyanagi, A. Romero-Rodríguez, and M. Sakellariadou, Phys. Rev. D **110**, 084063 (2024).
[66] M. Maggiore, Phys. Rept. **331**, 283 (2000).
[67] S. Mukherjee and J. Silk, Mon. Not. Roy. Astron. Soc. **491**, 4690 (2020).
[68] R. Buscicchio, C. J. Moore, G. Pratten, P. Schmidt, M. Bianconi, and A. Vecchio, Phys. Rev. Lett. **125**, 141102 (2020).
[69] M. R. Sah and S. Mukherjee, Mon. Not. Roy. Astron. Soc. **527**, 4100 (2023).
[70] M. R. Sah and S. Mukherjee, Phys. Rev. D **113**, 123058 (2026).
[71] J. Aasi, B. P. Abbott, R. Abbott, T. Abbott, M. R. Abernathy, K. Ackley, C. Adams, T. Adams, P. Addesso, R. X. Adhikari, and (The LIGO Scientific Collaboration), Class. Quantum Grav. **32**, 074001 (2015).
[72] F. Acernese, M. Agathos, K. Agatsuma, D. Aisa, N. Allemandou, A. Allocca, J. Amarni, P. Astone, G. Balestri, G. Ballardin, *et al.*, Class. Quantum Grav. **32**, 024001 (2014).
[73] T. Akutsu *et al.* (KAGRA), PTEP **2021**, 05A101 (2021).
[74] B. P. Abbott *et al.* (LIGO Scientific Collaboration, Virgo Collaboration, KAGRA Collaboration), Living Rev. Rel. **19**, 1 (2016).
[75] A. G. Abac *et al.* (LIGO Scientific Collaboration, Virgo Collaboration, KAGRA Collaboration), (2025), arXiv:2508.20721 [gr-qc].
[76] A. G. Abac, I. Abouelfettouh, F. Acernese, K. Ackley, C. Adamcewicz, S. Adhicary, D. Adhikari, N. Adhikari, R. X. Adhikari, V. K. Adkins, S. Afroz, *et al.* (LIGO Scientific Collaboration, Virgo Collaboration, KAGRA Collaboration), Phys. Rev. D **114**, 022001 (2026).
[77] A. G. Abac *et al.* (LIGO Scientific Collaboration, Virgo Collaboration, KAGRA Collaboration), (2025), arXiv:2510.26848 [gr-qc].
[78] B. Allen and J. D. Romano, Phys. Rev. D **59**, 102001 (1999).
[79] J. Romano and N. Cornish, Living Rev. Relativ. **20** (2017), 10.1007/s41114-017-0004-1.
[80] N. J. Cornish and J. D. Romano, Phys. Rev. D **92**, 042001 (2015).
[81] A. C. Jenkins, *Cosmology and Fundamental Physics in the Era of Gravitational-Wave Astronomy*, Ph.D. thesis, King's Coll. London (2022), arXiv:2202.05105 [gr-qc].
[82] H. Zhong, J. D. Romano, V. Mandic, S. Kandhasamy, and A. I. Renzini, (2026), arXiv:2606.23816 [gr-qc].
[83] A. G. Abac *et al.* (LIGO Scientific Collaboration, Virgo Collaboration, KAGRA Collaboration), (2026), arXiv:2605.27090 [gr-qc].
[84] LIGO Scientific Collaboration, Virgo Collaboration and KAGRA Collaboration, "LVK announces an update of the observing schedule," `https://www.virgo-gw.eu/news/lvk-announces-an-update-of-the-observing-schedule/` (2025), accessed: 2026-05-28.
[85] A. Matas and J. Romano, Phys. Rev. D **103** (2021), 10.1103/PhysRevD.103.062003.
[86] A. I. Renzini, A. Romero-Rodriguez, C. Talbot, M. Lalleman, S. Kandhasamy, K. Turbang, S. Biscoveanu, K. Martinovic, P. Meyers, L. Tsukada, K. Janssens, D. Davis, A. Matas, P. Charlton, G. chin Liu, and I. Dvorkin, Journal of Open Source Software **9**, 5454 (2024).
[87] A. I. Renzini, A. Romero-Rodriguez, C. Talbot, M. Lalleman, S. Kandhasamy, K. Turbang, S. Biscoveanu, K. Martinovic, P. Meyers, L. Tsukada, K. Janssens, D. Davis, A. Matas, P. Charlton, G. chin Liu, and I. Dvorkin, Astrophys. J. **952**, 25 (2023).
[88] E. Thrane, N. Christensen, and R. M. S. Schofield, Phys. Rev. D **87** (2013), 10.1103/physrevd.87.123009.
[89] E. Thrane, N. Christensen, R. Schofield, and A. Effler, Phys. Rev. D **90** (2014), 10.1103/physrevd.90.023013.
[90] K. Janssens *et al.*, Phys. Rev. D **107**, 022004 (2023).
[91] K. Janssens *et al.*, Phys. Rev. D **112**, 102003 (2025).
[92] M. W. Coughlin *et al.*, Class. Quant. Grav. **33**, 224003 (2016).
[93] M. W. Coughlin, A. Cirone, P. Meyers, S. Atsuta, V. Boschi, A. Chincarini, N. L. Christensen, R. De Rosa, A. Effler, I. Fiori, M. Gołkowski, M. Guidry, J. Harms, K. Hayama, Y. Kataoka, J. Kubisz, A. Kulak, M. Laxen, A. Matas, J. Mlynarczyk, T. Ogawa, F. Paoletti, J. Salvador, R. Schofield, K. Somiya, and E. Thrane, Phys. Rev. D **97**, 102007 (2018).
[94] K. Janssens, K. Martinovic, N. Christensen, P. M. Meyers, and M. Sakellariadou, Phys. Rev. D **104**, 122006 (2021), [Erratum: Phys.Rev.D 105, 109904 (2022)].
[95] A. Nishizawa, A. Taruya, K. Hayama, S. Kawamura, and M.-a. Sakagami, Phys. Rev. D **79**, 082002 (2009).
[96] T. Callister, A. S. Biscoveanu, N. Christensen, M. Isi, A. Matas, O. Minazzoli, T. Regimbau, M. Sakellariadou, J. Tasson, and E. Thrane, Phys. Rev. X **7**, 041058 (2017).
[97] T. Regimbau, Research in Astronomy and Astrophysics **11**, 21 (2011).
[98] A. G. Abac *et al.* (LIGO Scientific Collaboration, Virgo Collaboration, KAGRA Collaboration), (2026), arXiv:2605.27223 [gr-qc].
[99] A. G. Abac *et al.* (LIGO Scientific Collaboration, Virgo Collaboration, KAGRA Collaboration), (2026), arXiv:2605.27226 [astro-ph.HE].
[100] P. Fritschel, B. Kabagoz, B. Kuns, and A. Effler, "A+/O5 strain curve projections," `https://dcc.ligo.org/LIGO-T2500310/public` (2025).
[101] B. P. Abbott, R. Abbott, T. D. Abbott, M. R. Abernathy, F. Acernese, K. Ackley, C. Adams, T. Adams,

P. Addesso, R. Adhikari, *et al.* (LIGO Scientific Collaboration and Virgo Collaboration), Phys. Rev. Lett. **118**, 121101 (2017).
[102] B. P. Abbott, R. Abbott, T. D. Abbott, S. Abraham, F. Acernese, K. Ackley, C. Adams, V. B. Adya, C. Affeldt, Agathos, *et al.* (LIGO Scientific and Virgo Collaboration), Phys. Rev. D **100**, 061101 (2019).
[103] R. Abbott, T. D. Abbott, S. Abraham, F. Acernese, K. Ackley, A. Adams, C. Adams, R. X. Adhikari, V. B. Adya, C. Affeldt, *et al.* (LIGO Scientific Collaboration, Virgo Collaboration, and KAGRA Collaboration), Phys. Rev. D **104**, 022004 (2021).
[104] J. Glanzer *et al.*, (2026), arXiv:2608.12193 [astro-ph.IM].
[105] G. Vajente, Y. Huang, M. Isi, J. Driggers, J. Kissel, M. Szczepańczyk, and S. Vitale, Phys. Rev. D **101** (2020), 10.1103/physrevd.101.042003.
[106] E. Capote, W. Jia, N. Aritomi, M. Nakano, V. Xu, *et al.*, Phys. Rev. D **111** (2025), 10.1103/physrevd.111.062002.
[107] E. Goetz *et al.*, "Narrow spectral artifact investigation and mitigation in LIGO data from the fourth LIGO-Virgo-KAGRA observing run," (2026), arXiv:2606.05959 [astro-ph.IM].
[108] B. P. Abbott *et al.* (LIGO Scientific Collaboration, Virgo Collaboration, KAGRA Collaboration), Phys. Rev. Lett. **116**, 131103 (2016).
[109] W. O. Schumann, Z. Naturforsch. A **7**, 250 (1952).
[110] W. O. Schumann, Z. Naturforsch. A **7**, 149 (1952).
[111] P. Nguyen, R. M. S. Schofield, A. Effler, C. Austin, V. Adya, M. Ball, S. Banagiri, K. Banowetz, C. Billman, C. D. Blair, *et al.*, Class. Quantum Grav. **38**, 145001 (2021).
[112] I. Fiori, F. Paoletti, M. Tringali, K. Janssens, C. Karathanasis, A. Menéndez-Vázquez, A. Romero-Rodríguez, R. Sugimoto, T. Washimi, V. Boschi, A. Chiummo, M. Cieślar, R. De Rosa, C. Rossi, F. Di Renzo, I. Nardecchia, A. Pasqualetti, B. Patricelli, P. Ruggi, and N. Singh, Galaxies **8**, 82 (2020).
[113] P. Nguyen, R. M. S. Schofield, A. Effler, C. Austin, V. Adya, M. Ball, S. Banagiri, K. Banowetz, C. Billman, *et al.*, Class. Quantum Grav. **38**, 145001 (2021).
[114] E. Thrane and J. D. Romano, Phys. Rev. D **88**, 124032 (2013).
[115] L. Sun *et al.*, Class. Quant. Grav. **37**, 225008 (2020).
[116] L. Sun *et al.*, Class. Quantum Grav (2021), arXiv:2107.00129 [astro-ph.IM].
[117] S. Vitale, C.-J. Haster, L. Sun, B. Farr, E. Goetz, J. Kissel, and C. Cahillane, Phys. Rev. D **103**, 063016 (2021).
[118] J. T. Whelan, E. L. Robinson, J. D. Romano, and E. H. Thrane, J. Phys. Conf. Ser. **484**, 012027 (2014).
[119] J. Yousuf, S. Kandhasamy, and M. A. Malik, Phys. Rev. D **107**, 102002 (2023).
[120] C. Caprini and D. G. Figueroa, Class. Quant. Grav. **35**, 163001 (2018).
[121] P. M. Meyers, K. Martinovic, N. Christensen, and M. Sakellariadou, Phys. Rev. D **102**, 102005 (2020).
[122] A. G. Abac *et al.* (LIGO Scientific Collaboration, Virgo Collaboration, KAGRA Collaboration), (2026), arXiv:2605.27225 [gr-qc].
[123] LIGO Scientific Collaboration, Virgo Collaboration, KAGRA Collaboration, (2025), arXiv:2508.18083 [astro-ph.HE].
[124] M. Dominik, K. Belczynski, C. Fryer, D. E. Holz, E. Berti, T. Bulik, I. Mandel, and R. O'Shaughnessy, Astrophys. J. **779**, 72 (2013).
[125] A. P. Boesky, F. S. Broekgaarden, and E. Berger, Astrophys. J. **976**, 24 (2024).
[126] A. I. Renzini and J. Golomb, Astron. Astrophys. **691**, A238 (2024).
[127] M. Ebersold and T. Regimbau, Phys. Rev. D **113**, 044026 (2026).
[128] T. Callister, M. Fishbach, D. Holz, and W. Farr, Astrophys. J. Lett. **896**, L32 (2020).
[129] P. Madau and T. Fragos, Astrophys. J. **840**, 39 (2017).